



## RESEARCH ARTICLE

10.1002/2017JG004166

## Key Points:

- Eroding permafrost along the Yukon coast contributes 0.036 Tg of soil organic carbon to the Beaufort Sea annually
- In permafrost soils, large corrections to organic carbon contents are needed to properly account for the volume of ground ice
- More than half of the soil organic carbon in coastal bluffs is found at depths greater than 1 m

## Supporting Information:

- Supporting Information S1
- Table S1

## Correspondence to:

N. J. Couture,  
nicole.couture@canada.ca

## Citation:

Couture, N. J., Irrgang, A., Pollard, W., Lantuit, H., & Fritz, M. (2018). Coastal erosion of permafrost soils along the Yukon Coastal Plain and fluxes of organic carbon to the Canadian Beaufort Sea. *Journal of Geophysical Research: Biogeosciences*, 123, 406–422. <https://doi.org/10.1002/2017JG004166>

Received 20 SEP 2017

Accepted 18 JAN 2018

Accepted article online 24 JAN 2018

Published online 17 FEB 2018

## Coastal Erosion of Permafrost Soils Along the Yukon Coastal Plain and Fluxes of Organic Carbon to the Canadian Beaufort Sea

Nicole J. Couture<sup>1,2</sup> , Anna Irrgang<sup>3,4</sup> , Wayne Pollard<sup>2</sup>, Hugues Lantuit<sup>3,4</sup> , and Michael Fritz<sup>3</sup>

<sup>1</sup>Geological Survey of Canada, Natural Resources Canada, Ottawa, Ontario, Canada, <sup>2</sup>Department of Geography, McGill University, Montreal, Quebec, Canada, <sup>3</sup>Department of Periglacial Research, Alfred Wegener Institute Helmholtz Centre for Polar and Marine Research, Potsdam, Germany, <sup>4</sup>Institute of Earth and Environmental Science Potsdam, University of Potsdam, Potsdam, Germany, Canada

**Abstract** Reducing uncertainties about carbon cycling is important in the Arctic where rapid environmental changes contribute to enhanced mobilization of carbon. Here we quantify soil organic carbon (SOC) contents of permafrost soils along the Yukon Coastal Plain and determine the annual fluxes from coastal erosion. Different terrain units were assessed based on surficial geology, morphology, and ground ice conditions. To account for the volume of wedge ice and massive ice in a unit, SOC contents were reduced by 19% and sediment contents by 16%. The SOC content in a 1 m<sup>2</sup> column of soil varied according to the height of the bluff, ranging from 30 to 662 kg, with a mean value of 183 kg. Forty-four per cent of the SOC was within the top 1 m of soil and values varied based on surficial materials, ranging from 30 to 53 kg C/m<sup>3</sup>, with a mean of 41 kg. Eighty per cent of the shoreline was erosive with a mean annual rate of change of  $-0.7$  m/yr. This resulted in a SOC flux per meter of shoreline of 132 kg C/m/yr, and a total flux for the entire 282 km of the Yukon coast of  $35.5 \times 10^6$  kg C/yr (0.036 Tg C/yr). The mean flux of sediment per meter of shoreline was  $5.3 \times 10^3$  kg/m/yr, with a total flux of  $1,832 \times 10^6$  kg/yr (1.832 Tg/yr). Sedimentation rates indicate that approximately 13% of the eroded carbon was sequestered in nearshore sediments, where the overwhelming majority of organic carbon was of terrestrial origin.

**Plain Language Summary** The oceans help slow the buildup of carbon dioxide (CO<sub>2</sub>) because they absorb much of this greenhouse gas. However, if carbon from other sources is added to the oceans, it can affect their ability to absorb atmospheric CO<sub>2</sub>. Our study examines the organic carbon added to the Canadian Beaufort Sea from eroding permafrost along the Yukon coast, a region quite vulnerable to erosion. Understanding carbon cycling in this area is important because environmental changes in the Arctic such as longer open water seasons, rising sea levels, and warmer air, water and soil temperatures are likely to increase coastal erosion and, thus, carbon fluxes to the sea. We measured the carbon in different types of permafrost soils and applied corrections to account for the volume taken up by various types of ground ice. By determining how quickly the shoreline is eroding, we assessed how much organic carbon is being transferred to the ocean each year. Our results show that  $36 \times 10^6$  kg of carbon is added annually from this section of the coast. If we extrapolate these results to other coastal areas along the Canadian Beaufort Sea, the flux of organic carbon is nearly 3 times what was previously thought.

### 1. Introduction

It is estimated that  $1,035 \pm 150$  Pg ( $10^{15}$  g) of soil organic carbon (SOC) are stored in permafrost (Hugelius et al., 2014), which is approximately 20% more carbon than is currently circulating in the atmosphere (Houghton, 2007). Because permafrost is such an important global carbon sink, quantifying the carbon fluxes that result from its disturbance is crucial for understanding carbon cycling from local to global scales and for refining projections of future climatic changes (Fritz et al., 2017). Thirty four per cent of the Earth's coasts consist of permafrost (Lantuit et al., 2012), and these coasts have a mean erosion rate of 0.5 m/yr (Lantuit et al., 2012), with local retreat rates as high as 30 m/yr (Wobus et al., 2011). Consequently, coastal erosion is an important process for mobilizing organic carbon in permafrost regions, releasing an estimated 14.0 Tg ( $10^{12}$  g) of particulate organic carbon to the nearshore zone each year (Wegner et al., 2015). This carbon flux is comparable to that contributed annually by all Arctic rivers, or to the net methane (CH<sub>4</sub>) emissions from

©2018. American Geophysical Union and Her Majesty the Queen in Right of Canada. Reproduced with the permission of the Minister of Natural Resources Canada.

This is an open access article under the terms of the Creative Commons Attribution-NonCommercial-NoDerivs License, which permits use and distribution in any medium, provided the original work is properly cited, the use is non-commercial and no modifications or adaptations are made.

terrestrial permafrost (Koven et al., 2011). Terrestrially derived organic carbon plays a crucial role in Arctic biogeochemical cycling once released into the nearshore zone, where it can either be remineralized in the water column, buried on the shelf, or transported to the deep ocean (Fritz et al., 2017). Uncertainties remain about the carbon fluxes to and from the system, however, and reducing those uncertainties is especially critical in the Arctic, where rapid environmental changes due to Arctic amplification (Serreze & Barry, 2011) are likely to increase the cycling of carbon (McGuire et al., 2009; Schuur et al., 2008).

Studies of the overall cycling of organic carbon in the Arctic Ocean have progressed toward elucidating the processes involved and highlighting the knowledge gaps (Stein & Macdonald, 2004; Vetrov & Romankevich, 2004). On a volume basis, the Arctic Ocean receives higher levels of terrestrially derived organic matter than any other ocean (Dittmar & Kattner, 2003), with inputs from both riverine and coastal sources (Rachold et al., 2000, 2004). A major goal of the Arctic Coastal Dynamics project was to develop circum-Arctic estimates of the coastal contribution of sediment and carbon (Rachold et al., 2005). The coastal inputs of organic carbon from some regions are well constrained (Jorgenson & Brown, 2005; Ping et al., 2011; Rachold et al., 2004; Streletskaia et al., 2009), but uncertainty still exists for other areas. For the Canadian Beaufort Sea, inputs are largely dominated by discharge from the Mackenzie River (Macdonald et al., 1998). However, although several studies have provided estimates of material fluxes to the Beaufort Sea from coastal sources (Harper, 1990; Harper & Penland, 1982; Hill et al., 1991; Macdonald et al., 1998; McDonald & Lewis, 1973; Yunker et al., 1990, 1991, 1993), organic carbon inputs for this region are still not very well defined. Here we seek to address this gap by carrying out a systematic analysis to determine the sediment and carbon contents of soils along the Yukon Coastal Plain and fluxes to the Beaufort Sea.

The long-term mean rate of shoreline change along the Yukon coast is  $-0.7$  m/yr, with some parts of the coast having mean retreat rates as high as 9 m/yr (Irrgang et al., 2017). Along the north coast of Alaska, long-term rates of shoreline change are  $-1.4$  m/yr (Gibbs & Richmond, 2015). This region therefore has the potential to release high amounts of organic matter. In North America, total organic carbon (TOC) contents of permafrost soils have been shown to vary considerably depending on soil type and land cover (Bockheim et al., 1999, 2004, 1998, 2003; Bockheim & Hinkel, 2007; Michaelson et al., 1996; Obu, Lantuit, Myers-Smith, et al., 2017; Ping et al., 2008; Tarnocai, 1998; Tarnocai et al., 2003, 2007, 2009), with mean values between 30 and 60 kg C/m<sup>3</sup>. Most measurements of TOC in permafrost have been confined to the top 1 m of soil, although some recent studies have examined deeper deposits (Bockheim & Hinkel, 2007; Strauss et al., 2013; Tarnocai et al., 2009; Zimov et al., 2006). In Arctic soils, in general, most soil organic matter is stored in the seasonally unfrozen active layer near the ground surface, so organic matter tends to decrease with depth. However, a considerable amount of organic matter can be transferred into the upper part of permafrost through cryoturbation (Bockheim & Tarnocai, 1998). Along the Yukon Coastal Plain, measurements of TOC in soils have been conducted at only a few sites (Fritz et al., 2012; Kokelj et al., 2002; Obu, Lantuit, Myers-Smith, et al., 2017; Smith et al., 1989; Tarnocai & Lacelle, 1996; Yunker et al., 1990), yielding values between 2.9 and 99.2 kg C/m<sup>3</sup>.

A preliminary estimate of the flux of organic carbon, based on earlier studies of coastal erosion, provided a value of 0.055 Tg/yr (with a maximum of 0.3 Tg/yr) for the entire Canadian Beaufort Sea coast (Macdonald et al., 1998). However, although that study implicitly accounted for pore ice through the use of soil bulk densities in its calculations, it did not account for other ground ice types, despite the fact that ground ice represents a significant portion of earth materials along the Yukon coast (Couture & Pollard, 2017). The fate of mobilized carbon is not well constrained and potential off-shelf transport is especially important along the Yukon coast because, with a width of 40 km and even 10 km in some places, it is very narrow in comparison to other shelves of the Arctic Ocean. Although databases exist of organic carbon in offshore sediments of the Alaska Beaufort Sea (Naidu et al., 2000) and of the Mackenzie Shelf (Macdonald et al., 2004), they include only a few samples from the Yukon coastal area.

Environmental changes in the Arctic such as longer open water seasons (Jones et al., 2009; Markus et al., 2009; Stroeve et al., 2014), intensified storms (Manson & Solomon, 2007), warmer air, water, and soil temperatures (AMAP, 2017; Overland et al., 2015; Timmermans & Proshutinsky, 2016) and rising sea level (Manson & Solomon, 2007) are very likely to further increase coastal erosion (Günther et al., 2015; Zhang et al., 2004) and thus carbon mobilization (McGuire et al., 2009; Schuur et al., 2008, 2015). This trend is already becoming evident, with erosion rates along many parts of the Beaufort Sea coast more than doubling in recent decades

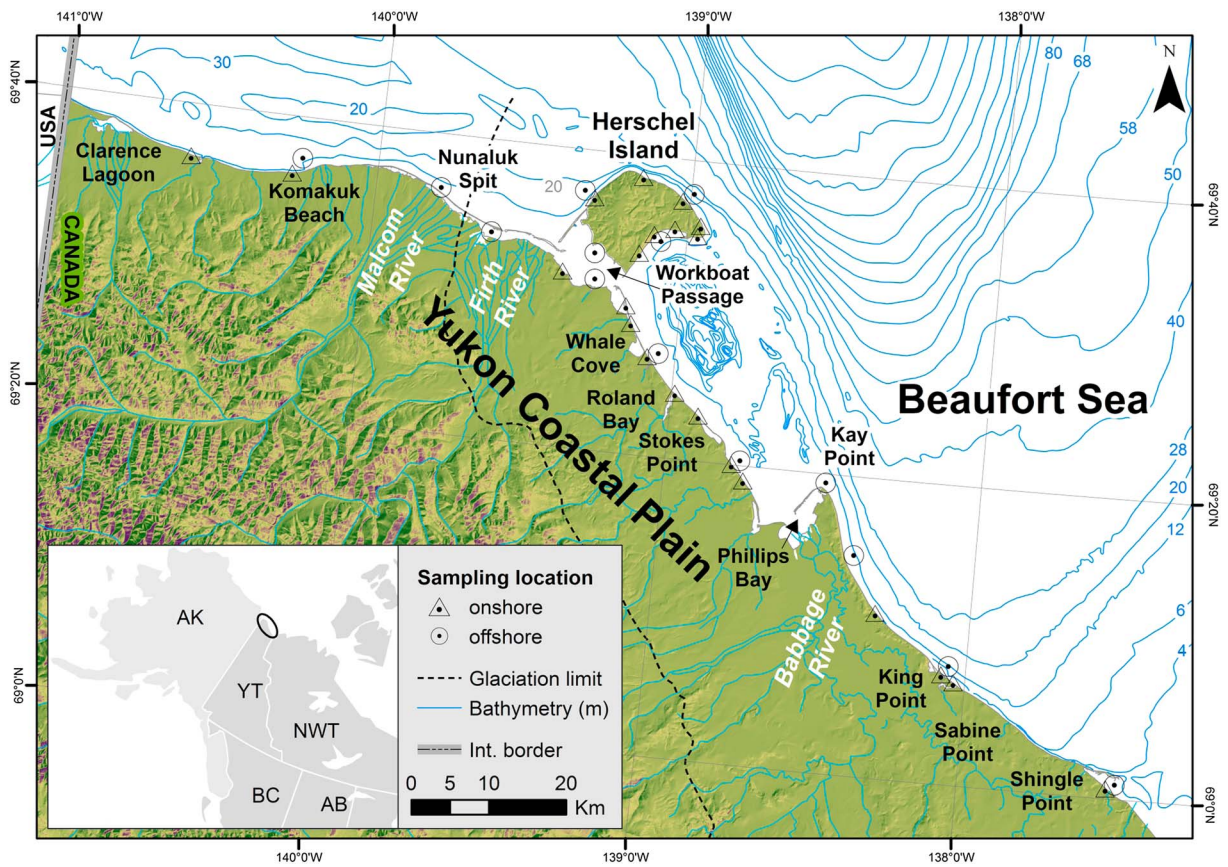


**Figure 1.** Map of the study area along the Yukon Coastal Plain, Canada. Samples of soil organic carbon (SOC) were collected at 22 onshore sites (γ) and 14 offshore (◁) sites. Bathymetry information is based on Canadian Hydrographic Survey navigational charts improved by local surveys performed in the 1980s (Thompson, 1994). Basemap: 30 m Yukon DEM, interpolated from the digital 1:50,000 Canadian Topographic Database (Yukon Department of Environment, 2016).

(Irrgang et al., 2017; Jones et al., 2009, Ping et al., 2011). In order to contribute to an enhanced understanding of the implications of these changes for carbon cycling in the Arctic, our objectives are (1) to quantify the annual fluxes of sediments and organic carbon from eroding permafrost along the Yukon coast, ensuring that ground ice volumes at different depths are taken into consideration and (2) to estimate the amount of terrestrially derived organic matter being sequestered in shelf sediments in this region of the Beaufort Sea.

## 2. Study Area

The study area is part of the Yukon Coastal Plain, a pediment surface 282 km long and 10–30 km wide that slopes gently from a series of inland mountain ranges to the Canadian Beaufort Sea (Figure 1). It was partially glaciated during the Wisconsinan Glaciation, with the Laurentide Ice Sheet extending just to the west of Herschel Island (Fritz et al., 2012; Rampton, 1982). This formerly glaciated area is characterized by a mixture of morainic deposits and coarse-grained glaciofluvial material, but low spits and fine-grained lacustrine and fluvial sediments occur as well (Bouchard, 1974; Rampton, 1982). Cliff heights are diverse, ranging from 2–3 m on the mainland across from Herschel Island to 60 m in the eastern part of the study area. In the region to the west of Herschel Island, which remained unglaciated, sediments are of lacustrine or fluvial origin and are mostly fine-grained (Rampton, 1982). Coastal cliff heights are more uniform in this western region, rising gently from about 3 m high near the glaciation limit to approximately 6 m near the Yukon-Alaska border (Kohnert et al., 2014; Obu, Lantuit, Fritz, Grosse, et al., 2016). An approximately 35 km long barrier spit and barrier island system comprised of sand and gravel beach deposits fronts the deltas of the Malcolm and Firth Rivers.

Permafrost is found everywhere throughout the Yukon Coastal Plain except under large lakes and rivers (Rampton, 1982). The mean annual air temperature at Komakuk Beach is  $-11^{\circ}\text{C}$ ; July is the warmest month

with a mean temperature of 7.8°C (1971–2000) (Environment Canada, 2016). Over the last 100 years (from the period 1899–1905 to 1995–2006), mean air temperatures along the Yukon coast have increased by 2.5°C and permafrost temperatures have increased by 2.6°C (Burn & Zhang, 2009). This part of Canada is one of the most ice-rich areas of the Arctic and the permafrost contains high amounts of ground ice in the form of pore ice and thin lenses, ice wedges, and bodies of massive ice, the latter occurring primarily in the formerly glaciated area. Overall, ground ice accounts for 46% by volume of earth materials in the study area (Couture & Pollard, 2017), but it can be as high as 74% in some coastal segments. The sediments along the Yukon Coastal Plain are also rich in organic material, and peat layers from 0.5 to 3.5 m thick blanket many of the deposits (Rampton, 1982). Much of this organic matter accumulated in thermokarst basins that were formed by melting of ground ice; the accumulation is further promoted by poor drainage and the low regional slope gradients, particularly in the western part of the Yukon Coastal Plain (Fritz et al., 2012; Rampton, 1982). A considerable amount of organic material along the Yukon Coastal Plain is also found at depth in preglaciated floodplain and deltaic sediments, and where surface organic matter appears to have been buried by glacial deformation (Rampton, 1982). Current active layers along the Yukon coast range in thickness from approximately 0.3 to 1.5 m (Burn, 1997; Fritz et al., 2012; Kokelj et al., 2002). However, at maximum active layer development during the early Holocene about 8,000 <sup>14</sup>C years before present, active layer thicknesses were up to 2.5 times present-day ones (Burn, 1997; Fritz et al., 2012; Kokelj et al., 2002), so organic material that originated in the paleo-active layer is found in that depth range.

Because of the high ground ice contents, thermoerosional processes play an important role in shaping the landscape along the Yukon Coastal Plain. These processes include the development of retrogressive thaw slumps (Lantuit & Pollard, 2005, 2008; Ramage et al., 2017; Wolfe et al., 2001) and cliff collapse due to wave notching (Hoque & Pollard, 2009, 2015). Sea ice in the region breaks up in late June and re-forms in early October (Galley et al., 2016), and coastal erosion and the resulting mobilization of sediment and carbon is concentrated in the 3.5 months of open water. The most common wind directions are from the southeast and the northwest, though most effective storms come from the northwest, peaking in October (Atkinson, 2005; Hill et al., 1991; Hudak & Young, 2002). Sea level rise along the Yukon coast is on average  $3.5 \pm 1.1$  mm/yr (Manson & Solomon, 2007). Astronomical tides are semidiurnal and in the microtidal range (0.3–0.5 m) (Héquette et al., 1995).

### 3. Methods

The Yukon coast was segmented into 44 different terrain units based on landforms, surficial material, permafrost conditions, and coastal processes, since each of these factors influences the amount and flux of SOC. For each of the terrain units, the flux of SOC was calculated from the measured TOC contents and the long-term rates of shoreline change for each terrain unit (Irrgang et al., 2017). Analyses of seabed sediments allowed a quantification of the terrestrially derived SOC being buried in the nearshore.

#### 3.1. Sample Collection and Laboratory Analyses

Onshore soil sampling was carried out at 22 locations along the coast in September 2003 and August 2004, 2005, 2006, and 2009 (Figure 1). Locations were selected to represent terrain units from different parts of the coast. Sampling west of Herschel Island was restricted by ice conditions in 2005, and coarse-grained units were not well represented due to difficulties associated with coring in gravelly and pebbly material. Samples were collected from the side of soil pits in the unfrozen active layer. After digging down to the underlying permafrost and cleaning away any thawed material, samples were obtained using a modified CRREL corer (7.5 cm inner diameter). In a limited number of cases (7% of samples), natural exposures were sampled by scraping thawed soil off the face of the exposure and using a hammer or an ax to cut out samples (approximately 1,000 cm<sup>3</sup>). During sampling, active layer thicknesses ranged from 0.25 to 0.90 m. Cores began at the base of the active layer and penetrated to a maximum of 2.04 m below the ground surface. Natural exposures were sampled to a depth of 5.8 m from the surface. At two sites, samples were taken from the base of bluffs and were assumed to be representative of the entire lower portion of the bluff. The frozen cores were subsampled every 5 cm or where there was a distinct change in material composition. Samples were weighed in the field, then freeze-dried and reweighed in the laboratory to determine ice content and bulk densities (based on frozen core volume or measurement of the sample block).

Offshore samples were obtained at 14 locations in July 2006 (Figure 1). A Ponar grab sampler was used to obtain samples from bottom sediments along profiles perpendicular to the shore. Sample size varied due to differences in substrate and water depths, but averaged about 1,000 cm<sup>3</sup>. Samples were taken at distances of approximately 30 m, 50 m, 100 m, 250 m, and 500 m from shore to assess how the composition of the organic carbon in the sediments changed.

Dried samples were sieved to produce a <2 mm fraction, with larger granules later reintegrated into grain size statistics. Grain size distribution was determined by laser particle sizing (Coulter LS 200) of organic-free subsamples (treated with 30% H<sub>2</sub>O<sub>2</sub>). Total carbon, TOC, and total nitrogen were measured using an Elementar Vario EL III elemental analyzer following sample pulverization and treatment with 10% HCl to remove carbonates. Samples were measured twice and the mean value was determined. Stable carbon isotopes were measured on carbonate-free samples using a Finnigan MAT Delta-S mass spectrometer equipped with a FLASH elemental analyzer and a CONFLO III gas mixing system. The δ<sup>13</sup>C<sub>org</sub> of the sample was reported in per mill relative to Vienna Pee Dee Belemnite (VPDB). The standard deviation (1σ) was generally better than δ<sup>13</sup>C = ±0.15‰.

### 3.2. Determination of SOC and Sediment Contents

For each terrain unit, the onshore SOC measurements were used to calculate the mass of SOC ( $M_C$ ) for a 1 m<sup>2</sup> soil column equal in depth to the mean bluff height. Heights were obtained from 2013 LiDAR data (1.0 m ground resolution and vertical accuracy of 0.15 ± 0.1 m) (Kohnert et al., 2014; Obu, Lantuit, Fritz, Grosse, et al., 2016; Obu, Lantuit, Grosse, et al., 2017) and, using the zonal statistics tool in ESRI ArcMap, a mean value for each terrain unit was established for an area 200 m inland of a shoreline that was digitized from 2011 satellite images (Digital Globe, 2014, 2016). For terrain units composed of gravel features such as barrier islands and spits, the mean terrain height was set to 1 m, except for one (Stokes Point), which was assigned a height of 1.9 m based on survey data from Forbes (1997).

Where more than one sampling site occurred in a terrain unit, TOC values of the same depth were averaged before calculating  $M_C$ . For terrain units that did not contain a sampling site, values were extrapolated from areas with similar surficial geology and permafrost conditions. A column's  $M_C$  was given by

$$M_C = \sum_{j=1}^n \rho_b \times h \times \%OC \quad (1)$$

where  $M_C$  is the mass of SOC in a soil column (kg/m<sup>2</sup>),  $\rho_b$  is the dry bulk density based on the original frozen volume (kg/m<sup>3</sup>),  $h$  is the thickness of a soil layer (m), and %OC is the percentage of TOC by weight in a unit layer. The layers were summed to arrive at a value for the entire soil column. A similar procedure was followed to obtain the mass of the mineral portion of the sediment:

$$M_S = \sum_{j=1}^n (\rho_b \times h) - M_C \quad (2)$$

where  $M_S$  is the mass of mineral sediment (kg/m<sup>2</sup>).

For  $M_C$ , the lowermost soil layer, which generally comprises the largest percentage of the bluff, was assigned the lowest measured value for organic carbon. In cases of high bluffs where this value did not appear representative of the lowermost layer, a default value of 0.792 (% wt) TOC was assigned. This was one of the lowest values measured in the course of this study and came from a sample at the base of the highest cliff in the study area. Where no surface layer sample was available, a 10 cm-thick organic layer was assumed, with a TOC content of 25%. This is a conservative estimate based on horizon data reported by Michaelson et al. (1996) and Bockheim et al. (1999, 2003). Sand and gravel beach deposits were assigned a TOC value of 1.8% based on measurements by Smith et al. (1989) and Lawrence et al., (1984). For grab samples that had no volume measurements (9% of samples), bulk density was estimated from gravimetric ice contents according to the following equation:

$$\rho_b = \frac{\text{mass of sediment}}{\text{volume of ice} + \text{volume of sediment}} = \frac{100}{\left(\frac{\theta_i}{\rho_i}\right) + \left(\frac{100}{\rho_p}\right)} \quad (3)$$

where  $\theta_i$  is the gravimetric ice content of the sample (% wt) and the mass of the sediment is therefore

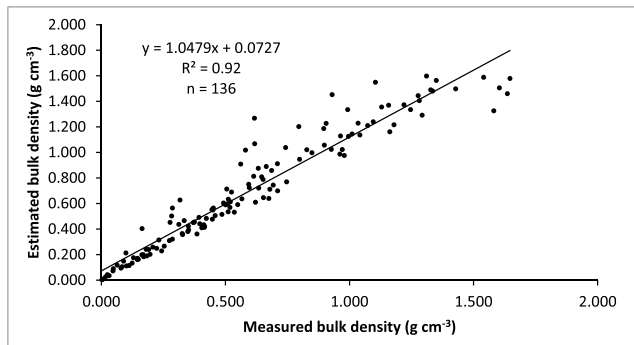


**Figure 2.** Correlation between measured bulk densities and bulk densities estimated from gravimetric ice contents.

assumed to be 100 g,  $\rho_i$  is the bulk density of ice (assumed to be 0.917 g/cm<sup>3</sup>), and  $\rho_p$  is the particle density of the sediment (assumed to be 2.6 g/cm<sup>3</sup>). There was a strong correlation ( $r^2 = 0.92$ ) when values estimated using this method were compared to measured values (Figure 2).

Where gravimetric ice contents were not available (35% of samples), another method was used based on several studies that showed a significant relationship ( $R^2 = 0.823$ ) between organic carbon concentrations and bulk densities (Bockheim et al., 1998, 2003). In those cases, bulk density was estimated according to the following empirically derived equation (Bockheim et al., 1998):

$$\rho_b = 1.374 (10^{-0.026x}) \quad (4)$$

where  $x$  is the TOC (% wt).

All SOC values were corrected to account for the volume occupied by wedge ice and massive ground ice in each layer within the column. Percentages of these ice types for each terrain unit are given by Couture (2010) and Couture and Pollard (2015, 2017) and details on the method used to estimate the different ground ice types are provided in Couture and Pollard (2017). These researchers found that pore ice and thin lenses of segregated ice comprise 35% of the volume of bluffs along the Yukon Coastal Plain, but corrections were not applied for these ice types, since they were already accounted for by the use of dry bulk density in the mass calculations.

### 3.3. Fluxes of SOC and Sediments

The following equation was used to calculate the annual SOC and sediment fluxes from shoreline retreat for an entire terrain unit:

$$F = A \left( \frac{M}{1,000} \right) \quad (5)$$

where  $F$  is the annual flux of SOC or sediment from the terrain unit (10<sup>3</sup> kg/yr),  $A$  is the mean annual area eroded per terrain unit (m<sup>2</sup>), and  $M$  is the total mass of material per soil column as defined above (equations (1) and (2)). Eroded area of the terrain units was used rather than shoreline length, since the use of length can result in scale-related errors of more than 30%, and using area provides results that are more robust (Lantuit et al., 2009).

For the determination of flux of SOC and sediment per meter of coast, mean annual rates of shoreline change for 35 of the terrain units were calculated for the period 1953–2011 (Irrgang et al., 2017). For the six terrain units on Herschel Island, mean annual rates of shoreline change were calculated following the same method, but for the period 1975–2011. Irrgang et al. (2017) were not able to determine rates of shoreline change for three of the terrain units (Running River, Kay Point Spit, and Malcolm River fan with barrier islands), so rates of change from Harper et al., (1985) were used. The mean rates of shoreline change were then multiplied by  $M_C$  and  $M_S$  in a 1 m<sup>2</sup> column to obtain annual fluxes per meter of coast for SOC and sediment, respectively. In two of the terrain units (Shingle Point E and Stokes Point SE), mean annual rates of shoreline change were positive, indicating net accumulation rather than erosion, but there was nevertheless some loss of sediment over the time period examined. For those two terrain units, a mean flux per meter of coast was therefore obtained by dividing the total annual loss from the terrain unit by the shoreline length of the unit (16.4 km and 4.1 km, respectively).

### 3.4. Fate of the Eroded SOC

In order to establish how much of SOC from the Yukon Coastal Plain is being sequestered in nearshore sediments, two bulk identifiers were examined in the seabed sediments: stable carbon isotopes ( $\delta^{13}C_{org}$ ) and organic carbon/total nitrogen (TOC/N) ratios. The amount of terrigenous organic carbon (TerrOC) in the bottom samples was determined from a mixing model that used the following equation, which assumes linear mixing between the terrigenous and marine sources of organic matter:

$$\text{TerrOC} = 100 \left( \frac{\delta^{13}\text{C}_{\text{sample}} - \delta^{13}\text{C}_{\text{marine}}}{\delta^{13}\text{C}_{\text{terrigenous}} - \delta^{13}\text{C}_{\text{marine}}} \right) \quad (6)$$

For the terrigenous end-member in equation (6),  $\delta^{13}\text{C}_{\text{org}}$  was measured directly in the onshore samples. The marine end-member can be quite variable in the Arctic due to phytoplankton and contributions from sea ice algae (Stein & Macdonald, 2004, and references therein). We used a value of  $-20.75\text{‰}$ , as this is the mean of the one proposed by Naidu et al. (2000) ( $-24\text{‰}$ ) and that used by Belicka and Harvey (2009) ( $-17.5\text{‰}$ ). The use of the TOC/N ratio helps to reduce uncertainty associated with the variability of the marine end-member.

## 4. Results

Of the 44 terrain units in the study area, TOC samples were collected directly from 17 terrain units. Results were extrapolated to a further 16 terrain units with similar characteristics, and in some cases, supplemented with stratigraphic information from previously published sources. For the marine units (i.e., beaches and spits) that we were unable to sample, TOC values reported in the literature were used.

### 4.1. Ground Ice

As noted earlier, pore ice and thin lenses of ground ice were accounted for in SOC calculations by the use of dry bulk densities, but other types of ground ice needed to be considered. The amount of wedge ice decreased with depth and ranged from a high of 53% of a soil layer's volume to less than 1%. Massive ice, although not present everywhere, accounted for between 52% and 97% of the volume in soil layers where it did occur. Applying corrections for the volume taken up by wedge ice and massive ice reduced overall SOC values by a mean of 19%, and sediment values by 16%. However, in terrain units with a high proportion of ground ice, reductions were as high as 43% for SOC and 46% for sediment. This underscores the importance of properly identifying and quantifying massive ice bodies in permafrost to accurately quantify carbon stocks and fluxes. Table 1 shows the specific reductions for each of the terrain units that contained wedge ice or massive ice.

### 4.2. Organic Carbon Contents

At the site level, TOC contents by percent weight generally decreased with depth. The mean for individual samples was 8.9% by weight, with a minimum of 0.5% and a maximum of 49.4%. When averaged over the entire soil column, the mean of all terrain units was  $4.5 \pm 3.6\%$ , with a range of 1.2–15.6%. The lowest values were seen in high bluffs with a significant mineral content (i.e., Herschel Island N, Herschel Island W) and the highest values were seen in low bluffs with a thick organic cover (i.e., Komakuk Beach). Once bulk densities (accounting for segregated ice) and corrections for wedge ice and massive ice were applied, the SOC and sediment contents and fluxes for all units were calculated. These are shown in Table 2. Across all units, the mean SOC content in a  $1 \text{ m}^2$  soil column was 183 kg. Values ranged from 30 to 662 kg  $\text{C}/\text{m}^2$  and generally increased with bluff height (Figure 3), as the volume under consideration increased. Within the top 1 m, the mean value was  $41 \pm 14 \text{ kg C}/\text{m}^3$ . Mean values varied based on surficial materials and were highest in fluvial deposits ( $53 \pm 15 \text{ kg C}/\text{m}^3$ ), followed by lacustrine ( $47 \pm 13 \text{ kg C}/\text{m}^3$ ), glaciofluvial ( $44 \pm 17 \text{ kg C}/\text{m}^3$ ), morainal ( $40 \pm 13 \text{ kg C}/\text{m}^3$ ), and finally marine ( $30 \pm 3 \text{ kg C}/\text{m}^3$ ). Analysis of variance (ANOVA) showed significant differences based on material type, but further testing (Tukey-Kramer HSD) revealed that only the marine unit showed a significant difference from the fluvial and the lacustrine groups (Figure 4). On average, the top meter contained  $43.8 \pm 33.0\%$  of the organic carbon in the entire soil column.

### 4.3. Material Fluxes

The mean annual rate of shoreline change for the 282 km long Yukon Coastal Plain was  $-0.7 \text{ m}/\text{yr}$ . Forty of the terrain units (comprising 80% of the shoreline) were undergoing erosion, two were accreting (6%), and two were stable (13%). Although fluxes from individual terrain units are provided in Table 2, it is the flux per meter of shoreline that is important for comparison between different parts of the coast, and between the Yukon coast and other regions in the circum-Arctic. The mean flux of SOC was 132 kg  $\text{C}/\text{m}/\text{yr}$ , with a maximum of 549 kg  $\text{C}/\text{m}/\text{yr}$  (Table 2, Figure 5). This resulted in a total flux of organic carbon from the Yukon coast of  $35.5 \times 10^6 \text{ kg}/\text{yr}$  ( $0.036 \text{ Tg}/\text{yr}$ ). The mean flux of sediment per meter of shoreline was  $5.3 \times 10^3 \text{ kg}/\text{m}/\text{yr}$ , with a maximum value of  $38.6 \times 10^3 \text{ kg}/\text{m}/\text{yr}$ , resulting in a total flux of sediment of  $1,832 \times 10^6 \text{ kg}/\text{yr}$  ( $1.832 \text{ Tg}/\text{yr}$ ).

**Table 1**
*Reduction in Values of Soil Organic Carbon and Sediment Due To the Presence of Wedge Ice and Bodies of Massive Ground Ice*

Terrain unit	Surficial geology <sup>a</sup>	Soil organic carbon (SOC)			Mineral sediment		
		Before correction (kg/m <sup>2</sup> )	After correction (kg/m <sup>2</sup> )	Reduction (%)	Before correction (kg/m <sup>2</sup> )	After correction (kg/m <sup>2</sup> )	Reduction (%)
Running River	F	578	560	3	24,559	24,218	1
Shingle Point E	Mm	249	212	15	16,342	15,169	7
Shingle Point W	Mm	443	252	43	25,008	21,158	15
Sabine Point E	L	514	321	38	6,996	5,566	20
Sabine Point	Mm	807	662	18	21,819	12,724	42
Sabine Point W	L	596	566	5	8,544	8,247	3
King Point SE	L	169	111	35	12,680	6,823	46
King Point	L	308	236	24	2,644	2,023	23
King Point NW	Mm	424	366	14	41,411	34,787	16
Kay Point SE	Mr	467	402	14	28,673	26,109	9
Kay Point	G	275	216	21	8,890	7,905	11
Phillips Bay	L	141	125	11	2,837	2,699	5
Phillips Bay NW	Mm	316	245	22	17,848	13,748	23
Stokes Point SE	L	195	161	17	6,539	6,352	3
Stokes Point W	Mm	301	240	20	15,343	12,165	21
Roland Bay E	L	221	210	5	10,267	9,825	4
Roland Bay W	Mm	203	150	26	9,123	6,541	28
Roland Bay NW	L	152	124	18	1,749	1,486	15
Whale Cove E	Mm	130	96	26	7,579	5,486	28
Whale Cove W	G	53	45	15	725	626	14
Workboat Passage E	G	68	50	26	1,142	861	25
Workboat Passage W	Mm	191	147	23	2,831	2,188	23
Herschel Island S	Mr	157	138	12	13,940	12,392	11
Herschel Island E	Mr	486	312	36	25,594	17,422	32
Herschel Island N	Mr	401	336	16	36,894	32,206	13
Herschel Island W	Mr	553	444	20	33,830	26,595	21
Malcolm River fan	F	71	67	6	2,058	1,829	11
Komakuk Beach	L	187	176	6	3,397	3,279	3
Komakuk W1	L	197	140	29	3,940	3,332	15
Komakuk W2	L	233	207	11	6,048	5,601	7
Clarence Lagoon E	F	78	73	5	2,421	2,189	10
Clarence Lagoon W	L	240	138	43	6,034	5,297	12
Mean		294	235	19	12,741	10,526	16
Minimum		53	45	3	725	626	1
Maximum		807	662	43	41,411	34,787	46

*Note.* Corrections are needed because volumes of wedge ice and massive ice were determined for the overall terrain unit, so were not accounted for within individual samples. The volume of each ice type was calculated for every sampled layer of soil and a correction applied to the measured values of SOC and sediment (see supporting information, Table S1). The results shown here are the summed values for all layers within a 1 m<sup>2</sup> soil column.

<sup>a</sup>Abbreviations for surficial geology: F = fluvial; Mm = rolling moraine; L = lacustrine; Mr = ice-thrust moraine; G = glaciofluvial.

#### 4.4. Organic Carbon in Nearshore Sediments

Analysis of 50 onshore samples taken from different terrain units gave a mean  $\delta^{13}\text{C}_{\text{org}}$  value of  $-27.12 \pm 0.77\text{‰}$ . This was the value used as the terrigenous end-member in the mixing model to determine the percentage of terrigenous organic carbon in the nearshore sediments. Samples of nearshore sediments were taken up to 500 m from shore and at water depths ranging from 0.9 to 14.5 m. Twenty-two of the nearshore samples were analyzed for  $\delta^{13}\text{C}_{\text{org}}$  ‰. Table 3 shows the results from isotopic analyses and from the mixing model. Three of the 22 samples should be viewed with caution because they showed very little decomposition visually and appeared to consist almost entirely of terrestrial organic matter, a fact corroborated by their low  $\delta^{13}\text{C}$  values and simultaneously high C/N ratios (Figure 6); these were omitted from further calculations. Values of  $\delta^{13}\text{C}$  for the nearshore samples ranged from  $-27.00$  to  $-26.10\text{‰}$  and C/N ratios ranged from 11.3 to 25.9. Based on results from the isotopic mixing model, the organic carbon in the nearshore sediments was overwhelmingly terrestrial, with a mean terrigenous organic carbon content of 91.3% and a marine content of 8.7%.

**Table 2**  
Terrain Unit Characteristics and Material Fluxes

Terrain unit	Bluff Height (m)	Change rate (m/yr)	Mean annual eroded area (m <sup>2</sup> /yr)	Soil organic carbon (SOC)					Mineral sediment			
				M <sub>c</sub> in 1 m <sup>2</sup> column (kg)	M <sub>c</sub> in top 1 m (kg)	M <sub>c</sub> > 1 m (kg)	C in top m (%)	M <sub>c</sub> flux per m of coast (kg/yr)	M <sub>c</sub> flux from unit (10 <sup>3</sup> kg/yr)	M <sub>s</sub> in 1 m <sup>2</sup> column (10 <sup>3</sup> kg)	M <sub>s</sub> Flux per m of coast (10 <sup>3</sup> kg/yr)	M <sub>s</sub> flux from unit (10 <sup>3</sup> kg/yr)
1. Running River	22.6	-0.7	2,827	560	59	501	11	392	1,583	24.2	17.0	68,463
2. Shingle Point E	13.7	0.2	3,103	2,12	34	1,78	16	40	6,58	15.2	0.0	47,070
3. Shingle Point W	21.1	-0.2	1,995	252	35	217	14	50	503	21.2	4.2	42,211
4. Sabine Point E	19.0	-0.4	894	321	46	275	14	114	287	5.6	2.0	49,76
5. Sabine Point	20.6	-0.8	2,000	662	59	604	9	549	1,324	12.7	10.6	25,448
6. Sabine Point W	20.6	-0.7	1,958	566	46	519	8	406	1,108	8.2	5.9	16,148
7. King Point SE	10.2	-1.1	4,057	111	31	80	28	117	449	6.8	7.2	27,682
8. King Point	7.4	-0.6	945	236	40	195	17	136	223	2.0	1.2	1,912
9. King Point Lagoon	1.0	-0.3	598	30	30	0	100	9	18	1.6	0.5	984
10. King Point NW	32.7	-0.2	686	366	40	326	11	78	251	34.8	7.4	23,864
11. Kay Point SE	26.1	-0.2	3,863	402	29	373	7	83	1,554	26.1	5.4	100,860
12. Kay Point	8.5	-2.3	5,972	216	63	153	29	496	1,290	7.9	18.2	47,210
13. Kay Point spit	1.0	0.0	0	30	30	0	100	0	0	1.6	0.0	0
14. Babbage River delta	3.2	-1.0	12,184	159	72	88	45	152	1,942	2.7	2.6	32,974
15. Phillips Bay	4.7	-0.6	6,545	125	47	78	38	81	815	2.7	1.7	17,666
16. Phillips Bay W	1.0	-0.5	3,154	34	34	0	100	17	106	1.6	0.8	51,77
17. Phillips Bay NW	13.8	-0.4	1,011	245	28	217	11	92	248	13.7	5.2	13,899
18. Stokes Point SE	8.3	0.5	408	161	42	120	26	16	66	6.4	0.0	2,592
19. Stokes Point	1.9	-3.6	16,989	57	30	27	53	204	973	3.1	11.1	53,094
20. Stokes Point W	12.5	-0.9	2,556	240	57	183	24	212	613	12.2	10.8	31,094
21. Roland Bay E	8.4	-0.7	1,733	210	24	186	11	157	364	9.8	7.4	17,026
22. Roland Bay W	8.4	-0.4	1,209	150	55	95	37	67	181	6.5	2.9	7,908
23. Roland Bay NW	5.9	-0.3	909	124	43	81	35	41	113	1.5	0.5	1,351
24. Whale Cove E	8.2	-0.2	150	96	18	78	18	17	14	5.5	1.0	823
25. Whale Cove W	1.7	-1.0	3,685	45	36	9	79	45	167	1.6	0.6	2,306
26. Whale Cove W	1.4	-0.3	2,156	42	30	12	72	12	91	2.3	0.7	4,965
27. Catton Point	2.3	-0.4	4,284	50	33	18	65	19	215	0.9	0.3	3,688
28. Workboat Passage E	6.4	-0.5	857	147	42	105	28	72	126	2.2	1.1	1,875
29. Workboat Passage W	11.0	-0.3	4,604	138	36	102	26	41	636	12.4	3.7	57,055
30. Herschel Island S	21.8	-0.4	4,365	312	34	278	11	125	1,360	17.4	7.0	76,048
31. Herschel Island E	1.0	-0.5	2,322	30	30	0	100	15	70	1.6	0.8	3,819
32. Simpson Point	36.0	-1.2	21,261	336	30	306	9	403	7,138	32.2	38.6	684,737
33. Herschel Island N	27.7	-0.9	6,064	444	55	389	12	400	2,695	26.6	23.9	161,271
34. Herschel Island W	1.2	-0.7	5,283	36	30	6	83	25	191	2.0	1.4	10,428
35. Avadlek spit	1.0	-1.2	27,180	30	24	6	80	36	819	1.6	2.0	44,707
36. Nunaliuk spit	1.0	0.0	0	30	30	0	100	0	0	1.6	0.0	0
37. Malcolim River fan with barrier islands	1.9	-0.8	7,211	67	51	16	76	54	481	1.8	1.5	13,189
38. Malcolim River fan	6.2	-1.3	17,377	176	63	113	36	236	3058	3.3	4.4	56,974
39. Komakuk Beach	6.8	-1.6	2,894	140	64	76	45	223	405	3.3	5.3	9,642
40. Komakuk W1												

Table 2. (continued)

Terrain unit	Bluff Height (m)	Change rate (m/yr)	Mean annual eroded area (m <sup>2</sup> /yr)	Soil organic carbon (SOC)					Mineral sediment			
				$M_c$ in 1 m <sup>2</sup> column (kg)	$M_c$ in top 1 m (kg)	$M_c > 1$ m (kg)	C in top m (%)	$M_c$ flux per m of coast (kg/yr)	$M_c$ flux from unit (10 <sup>3</sup> kg/yr)	$M_s$ in 1 m <sup>2</sup> column (10 <sup>3</sup> kg)	$M_s$ Flux per m of coast (10 <sup>3</sup> kg/yr)	$M_s$ flux from unit (10 <sup>3</sup> kg/yr)
41. Komakuk W2	6.7	-1.1	8,982	207	61	146	30	237	1,859	5.6	6.4	50,311
42. Clarence Lagoon E	2.2	-0.9	891	73	51	22	69	65	65	2.2	1.9	1,950
43. Clarence Lagoon	1.0	-0.8	2,738	30	30	0	100	25	83	1.6	1.4	4,504
44. Clarence Lagoon W	7.1	-1.6	9,779	138	61	77	44	215	1,347	5.3	8.3	51,798
Mean	9.7	-0.7	4,751.4	183	41	142	44	132	808	8.2	5.3	41,636
Minimum	1.0	-3.6	0.0	30	18	0	7	0	0	0.6	0.0	0
Maximum	36.0	0.5	27,180.0	662	72	604	100	549	7,138	34.8	38.6	684,737
Total flux (10 <sup>3</sup> kg/yr)									35,530			1,831,972

Note. The values for the mass of soil organic carbon ( $M_c$ ) and mineral sediment ( $M_s$ ) shown here have been corrected for the presence of ground ice.

## 5. Discussion

### 5.1. Ground Ice

As was seen from the reduction of SOC and sediment values in Table 1, failing to account for ground ice can result in significant overestimates of the total amount of material contained within a terrain unit and of its annual flux. Although wedge ice has been shown to account for 4% of frozen materials along the Yukon Coastal Plain (Couture & Pollard, 2017), it comprised 16% of the upper 7 m of soil. It is therefore not just the overall volume of ground ice that is important, but the stratigraphic relationship between wedge ice and organic carbon, in particular, since they both vary with depth (Couture & Pollard, 2017; Ulrich et al., 2014). In addition, several studies have noted the relationship between ground ice volumes and surficial deposits, with ground ice generally higher in fine-grained materials with higher SOC contents (e.g., Couture & Pollard, 2017; Kanevskiy et al., 2013; Rampton, 1982). Some studies, while acknowledging the importance of ground ice, do not include it in their calculations of material fluxes (i.e., Harper & Penland, 1982; Hill et al., 1991). Others considered ground ice volumes in varying degrees of detail. Our values for wedge ice are approximately twice those of Jorgenson and Brown (2005) who used a slightly cruder ice wedge geometry in their calculations of SOC contents for the Alaska Beaufort Sea coast. Brown et al. (2003) used a mean value of 50% for all ground ice types in the same region. In their analysis of TOC fluxes along the Alaskan Beaufort coast, Ping et al. (2011) used ice contents reported by Kanevskiy et al. (2013), who found a total average volumetric ice content of 77% (for wedge, segregated, and pore ice), with wedge ice ranging from 3 to 50% (mean 11%) within the top 3–4 m of various terrain types. Rachold et al. (2000) used different values for different coastal types along the Laptev Sea; some were simple means, while other were based on the various types of ground ice. Dallimore et al., (1996) provided an in-depth evaluation of all types of ice in their calculations of sediments fluxes from northern Richards Island in the Mackenzie Delta. In some cases, the importance of a detailed investigation depends on the geomorphology of the coast. For instance, Brown et al.'s (2003) use of a mean ground ice value of 50% did not have a significant impact on potential stratigraphic differences because the mean elevation of bluffs they considered was only 2.5 m, so changes in ice content or in SOC content with depth were not as important. Considering the varied elevations along the Yukon coast and the wide range of ground ice volumes with depth, our detailed stratigraphic approach is warranted.

### 5.2. Organic Carbon Contents

Given the sparseness of data on SOC for the Yukon Coastal Plain, this study contributes to a more thorough estimate of C stores in a region where carbon cycling is likely to increase with accelerating coastal erosion (Irrgang et al., 2017; Obu, Lantuit, Fritz, Pollard, et al., 2016; Radosavljevic et al., 2016). In addition to nearly tripling the number of pedons for which data are available, the results provide important information about deeper stores of organic carbon. The overall mean SOC value reported here (183 kg C/m<sup>2</sup>) is approximately 3 to 6 times higher than many previous estimates of TOC primarily because this study examines the entire soil column, whereas previous ones focused on the upper portions. Our values are closer to those reported by Jorgenson et al. (2003) in coastal banks up to 3.3 m high in northeastern Alaska (54 to 136 kg C/m<sup>2</sup>) or by Hugelius et al. (2014) who looked at depths up to 3 m and found organic carbon contents of 150 kg C/m<sup>2</sup> in the Arctic coastal lowlands. Dou et al. (2010), however, noted the spatial variability of SOC contents along the Alaskan Beaufort coast, reporting a range of 2.6 to 187 kg C/m<sup>2</sup> (mean 41.7 kg C/m<sup>2</sup>), with lower values in the east near the Canadian border. When comparing the top 1 m of soil only, our mean value of 41 kg C/m<sup>3</sup> is consistent with values found by Jorgenson and Brown (2005) for the entire Alaskan coast (30 to 79 kg C/m<sup>3</sup>). Bockheim et al. (1999) reported values of (50 kg C/m<sup>3</sup>) for the area around Barrow in northwestern Alaska coast. As they noted, this is less than other inland Arctic sites (62 kg C/m<sup>3</sup> reported in Michaelson et al., 1996, and

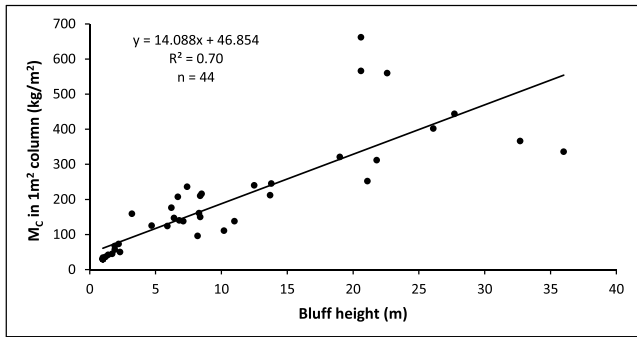


**Figure 3.** Correlation between bluff height and the mass of soil organic carbon ( $M_C$ ) in a  $1\text{ m}^2$  column.

65 kg C/m<sup>3</sup> in Bockheim et al., 1998), which might be due to higher ground ice contents in the coastal regions. Our results emphasize how important it is to include deeper carbon in calculations since only 44% of the SOC in our study was stored in the upper 1 m, with 56% of it at greater depths. Bockheim and Hinkel (2007) found 64% of SOC within the upper 1 m and 36% in the 1–2 m depth range. Tarnocai et al. (2009) calculated 48% for the upper 1 m, and 52% between 1 and 3 m; when they included even deeper deposits, the ratio became 30% SOC above 1 m to 70% below. A number of different processes have contributed to the presence of organic carbon at depth in the sediments of the Yukon Coastal Plain including cryoturbation, alluvial deposition, ice thrusting, accumulation in lacustrine basins, and possibly burial by eolian deposition (Rampton, 1982). Coastal erosion involves the mobilization of all

the carbon in the soil column relative to the sea level, so it is essential to consider deep SOC in flux calculations. In more inland regions, processes that affect carbon cycling (such as the thaw of the upper part of permafrost), are more likely to involve near-surface SOC only, so the consideration of carbon at greater depths may not be as critical. Several of the assumptions made in this study are conservative, particularly with regards to the 25% organic carbon content in the surface horizon and in extrapolating the values of 0.792% to the base of soil columns. In addition, the amount of carbon in some ice-thrust morainal units was likely underestimated since a minimum SOC value was used for most of the volume of the bluff, but glaciotectonic and thaw slump activity likely resulted in an interlayering of carbon-rich and carbon-poor layers.

**5.3. Material Fluxes**

The results presented here indicate fluxes of SOC (0.036 Tg/yr) and sediment (1.832 Tg/yr) from the 282 km of the Yukon Coastal Plain shoreline. The sediment flux is 17% more than the value given by earlier studies by Harper and Penland (1982) for the Yukon (and later used by Hill et al., 1991). Those authors noted that their sediment flux was a first approximation only and was likely a maximum value since they were not accounting for ground ice volumes. The discrepancy with our results is partly due to the fact that their study considered less of the shoreline to be erosive (150 km versus the approximately 225 km considered here) and partly due to probable differences in bluff height estimation. The only other study of SOC flux for the region was based on the entire shoreline of the Canadian Beaufort Sea (Macdonald et al., 1998) and provided a range of potential fluxes. Using data from Yunker et al. (1991), Macdonald et al. estimated annual flux to be 0.06 Tg/yr. Their value for the Yukon coast would be 0.015 Tg/yr, which is less than half of the flux found in this study. Again, they considered a shorter length of shoreline and only looked at eroding peat, not other sediment contained in the coastal bluffs. Their maximum estimate for SOC flux was 0.3 Tg/yr, based on data from Hill et al. (1991) and a presumed SOC content for all coastal sediments of 5% by weight. The value for the Yukon portion of the coast would be 0.12 Tg/yr, which is 3.5 times our result. As seen above, however, eroded volumes did not account for ground ice and so are likely too high. It is interesting to note that even though SOC values for our terrain units ranged from 1.2% to 15.6%, the value assumed by Macdonald et al. (1998) is very similar to our mean of 4.5% for all units. If our results from the Yukon Coastal Plain are applied to the other areas of peat erosion examined by Macdonald et al. (1998), the mean flux of SOC to the Canadian Beaufort Sea would be 0.17 Tg/yr, which is almost 3 times the value used to date in Arctic Ocean budgets (Rachold et al., 2004). This is

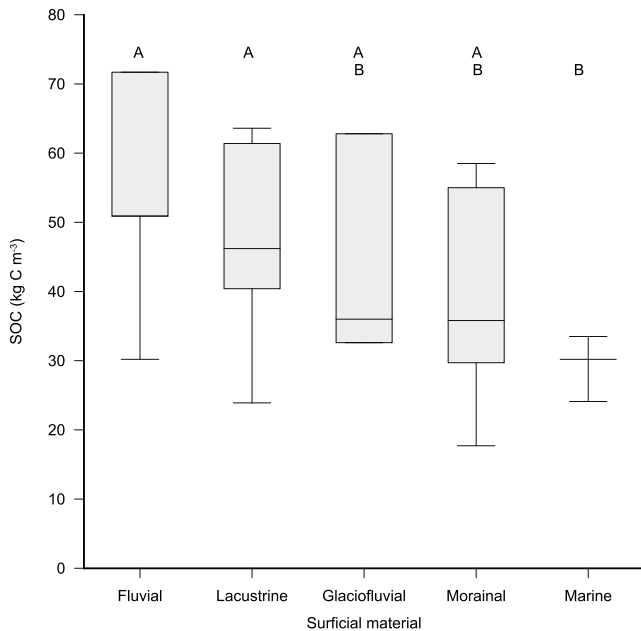


**Figure 4.** Soil organic carbon density in the top 1 m for terrain units with different surficial geologies. The line in the middle of boxes represents the median, with lower and upper parts of the box representing 25% and 75% of the distribution, while the lower and upper whiskers represent the minimum and maximum of the distribution. Materials not sharing the same letter above the box plots are significantly different from each other based on the Tukey–Kramer HSD comparison of means ( $p < 0.05$ ).

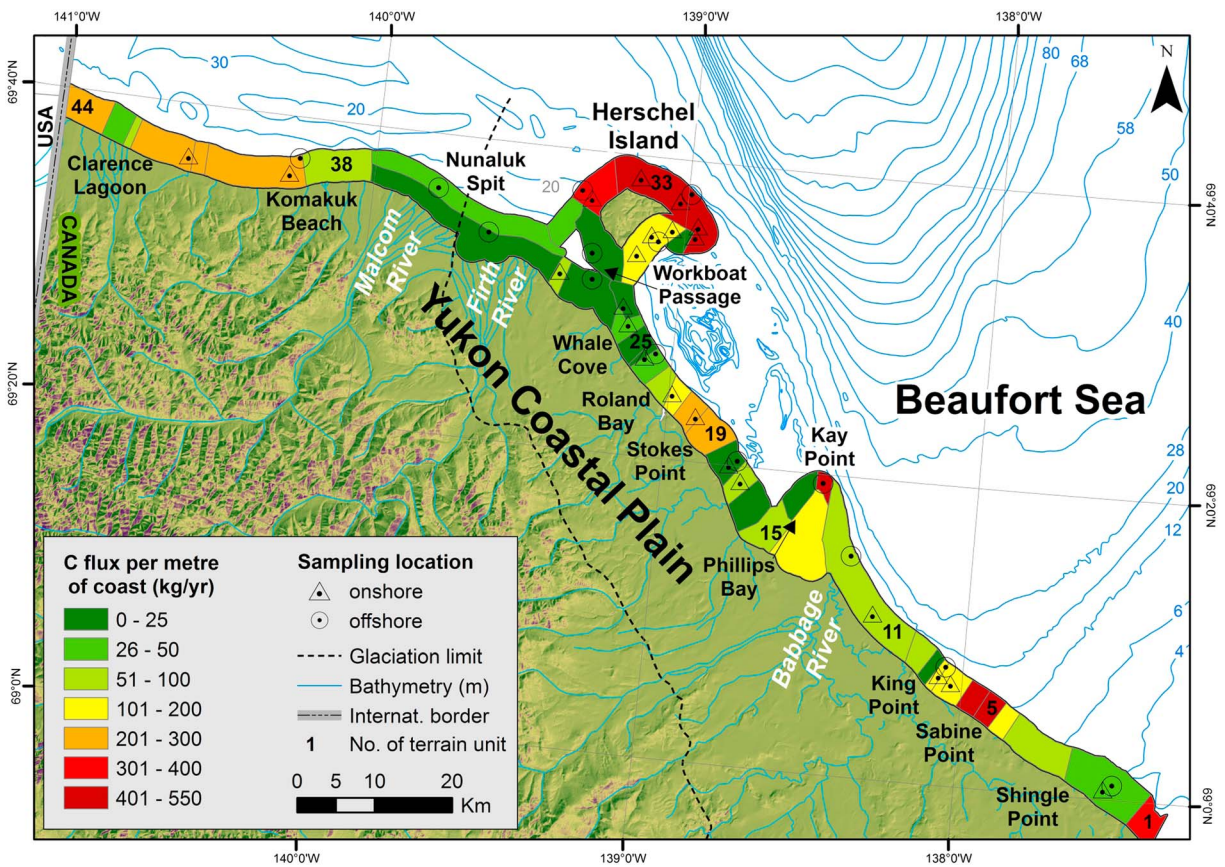


Figure 5. Annual flux of soil organic carbon per meter of coastline. Details on terrain unit characteristics are listed in Table 2.

approximately 10% of the particulate organic carbon input by the Mackenzie River each year (Hilton et al., 2015; Macdonald et al., 1998), which has the largest carbon input of any Arctic river (Rachold et al., 2004).

The flux of SOC per meter of shoreline found in this study (132 kg C/m) is intermediate to the results of studies for other Arctic Seas. Along the Alaskan Beaufort coast, estimates of the mean annual flux range from 73 kg C/m (Ping et al., 2011) to 149 kg C/m (Jorgenson & Brown, 2005), while results from Streletskaia et al. (2009) for the Kara Sea indicate a flux of 154 kg C/m. Rachold et al. (2004) found a mean of 263 kg C/m for different coastal types along the Laptev Sea and 375 kg C/m for the East Siberian Sea. Sediment fluxes show similar trends for the different seas. The lower values for the Alaskan Beaufort and Kara Seas appear to be the result of lower bluffs and lower SOC contents, respectively. The higher fluxes from the Laptev and East Siberian Seas are chiefly the result of higher erosion rates (Vonk et al., 2012).

Finally, it should be noted that the calculations in this study only involved subaerial erosion, although, over time, a significant amount of material can be eroded below the waterline (Are, 1988; Reimnitz et al., 1988; Vonk et al., 2012). This is primarily due to the paucity of data available for the nearshore along the Yukon Coastal Plain.

#### 5.4. Organic Carbon in Nearshore Sediments

Our results for carbon in nearshore sediments (91.3% terrigenous and 8.7% marine) are similar to those of Vonk et al. (2012) who found that marine organic carbon constituted 7% of nearshore shelf sediments in the East Siberian Sea. The influence of the value for the marine end-member in the mixing model can be seen by examining some of the values invoked in the literature. If we had chosen a

**Table 3**  
Properties of Nearshore Sediment Samples

Sample	Distance from shore (m)	Water depth (m)	TOC (%)	C/N ratio	$\delta^{13}C_{org}$ (‰ VPDB)	Terrigenous OC (%)
01-06	500	10.6	0.630	20.3	-26.86	95.9
03-06	100	3.7	0.979	11.9	-26.10	84.0
05-06	30	1.9	1.013	11.3	-26.21	85.7
06-06	500	14.5	0.829	18.0	-26.44	89.4
13-06	110	2.3	1.384	16.2	-26.91	96.7
15-06	500	2.7	1.375	20.1	-26.59	91.7
20-06	500	7.6	1.175	15.3	-27.00	98.1
27-06	250	1.2	1.014 <sup>a</sup>	18.6 <sup>a</sup>	-27.07 <sup>a</sup>	99.2 <sup>a</sup>
29-06	50	3.0	0.661 <sup>a</sup>	16.3 <sup>a</sup>	-27.19 <sup>a</sup>	>100 <sup>a</sup>
30-06	30	2.0	15.317 <sup>a</sup>	45.1 <sup>a</sup>	-27.86 <sup>a</sup>	>100 <sup>a</sup>
33-06	500	5.0	0.275	12.2	-26.69	93.2
38-06	30	3.8	0.861	13.4	-26.99	98.0
42-06	500	9.6	7.877	25.9	-26.72	93.7
45-06	250	5.2	1.142	14.0	-26.44	89.4
46-06	500	8.0	1.074	11.5	-26.52	90.5
47-06	30	2.3	1.853	13.5	-26.67	93.0
49-06	100	2.3	1.809	13.4	-26.37	88.3
51-06	500	2.5	1.944	13.1	-26.49	90.1
55-06	120	2.9	2.218	14.5	-26.58	91.4
57-06	500	2.7	1.435	15.0	-26.58	91.5
58-06	30	0.9	1.269	14.0	-26.31	87.3
62-06	500	6.7	0.801	12.4	-26.22	85.8
Mean			1.6	15.1	-26.6	91.3
Minimum		0.9	0.3	11.3	-27.0	84.0
Maximum		14.5	7.9	25.9	-26.1	98.1

<sup>a</sup>Samples omitted from calculation of means, maxima, and minima because of unusually high terrigenous content.

heavier value of -17.5‰ proposed by Belicka and Harvey (2009), the proportion of terrigenous carbon would have been 94%. Using the lighter value (-24.0‰) for the marine end-member suggested by Naidu et al. (2000) would have resulted in a mean terrigenous OC value of 82%. Belicka and Harvey (2009) compared several different methods of estimating terrestrial organic carbon, including the isotopic mixing model. Although each of the four proxy methods they examined produced different results, the mixing model, despite its sensitivity to the marine end-member, produced intermediate results. Because of the variability of the marine end-member, C/N ratios were used here to help in assessing the source of organic carbon in nearshore sediments. Figure 6 shows a plot of these two parameters for the nearshore samples. Although most samples were heavier than the terrigenous end-member, indicating a marine influence, the high C/N ratios helped to confirm the strong contribution of terrigenous carbon to these samples. Previous studies of organic carbon in the Beaufort Sea showed a progressive decrease in the terrigenous component as distance from shore increases (Macdonald et al., 2004; Naidu et al., 2000). No obvious trend was seen in our data set when comparing terrigenous carbon contents with distance from shore, likely due to the fact that the maximum distance from shore was limited to 500 m. However, it is interesting to note that the two samples with the highest marine content (open circles in Figure 6) were taken north of Herschel Island; although this area had one of the highest fluxes of C per meter of shoreline, it is farthest from the mainland, and therefore most likely to be subject to marine influences. Several studies show an overall shift toward heavier  $\delta^{13}C$  values from east to west in the Beaufort Sea due to decreased influence of the Mackenzie River and to the greater importance of

marine productivity in the more nutrient-rich waters in the west (Dunton et al., 2006; Naidu et al., 2000). Our data are consistent with that trend and are intermediate between values measured on the Mackenzie Shelf to the east and the Alaskan shelf to the west (Goñi et al., 2000; Macdonald et al., 2004; Naidu et al., 2000).

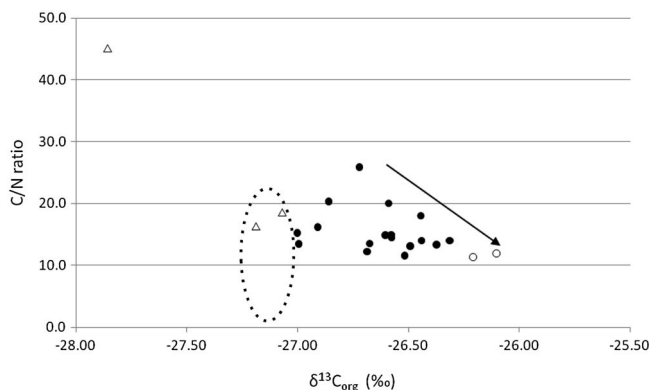


**Figure 6.** A plot displaying the relationship between C/N ratios and  $\delta^{13}C_{org}$  for seabed samples from the nearshore zone along the Yukon Coastal Plain. Open triangles represent three samples that showed very little decomposition and consist almost entirely of terrestrial organic matter. The dashed circle shows where a typical terrigenous end-member would be found, while the arrow indicates increasing marine organic matter content. The open circles represent samples with the highest marine content, taken north of Herschel Island.

Knowing how much of the OC in the nearshore sediments is of terrestrial origin provides an indication of how much of the annual flux is being sequestered in those sediments and how much may be remineralized or exported off-shelf. Following Macdonald et al. (1998), we estimated OC burial based on sedimentation rate and the proportion of OC in marine sediments. Sedimentation rates for the area adjacent to the Mackenzie Delta are relatively well known, but there is very little information for the shelf area to the west. Based on data from Harper and Penland (1982), rates range from 2 mm/yr near the delta to less than 0.1 mm/yr in more distal areas. If we use the lower value of sedimentation and assume a solid density of 2.6 g/cm<sup>3</sup> and a porosity of 60% for the marine sediments, then the annual flux of material to the seafloor for the entire shelf off the Yukon coast (which covers an area of 3,100 km<sup>2</sup> according to Macdonald et al., 1998) would be 0.32 Tg/yr. Of this, 1.5% was OC based on our measurements, 91.7% of which was of terrestrial origin. Therefore, 0.004 Tg or 12.2% of the OC eroded from the coastal sediments is sequestered in the nearshore sediments. This estimation requires validation based on extensive <sup>210</sup>Pb/<sup>137</sup>Cs dating of sediment cores from the shelf, comparable to the approach used by Vonk et al. (2012). The OC not sequestered in the

nearshore is mineralized or transported off the shelf (de Haas et al., 2002; Hedges et al., 1997). There is strong support that terrigenous OC is involved in both processes. For instance, a considerable amount of terrigenous material has been found in sediment traps at the shelf edge (O'Brien et al., 2006) and beyond (Belicka et al., 2002, 2009; Stein & Macdonald, 2004), and Dunton et al. (2006) demonstrate that terrigenous OC may constitute up to 70% of the dietary requirements of species in the nearshore along the Alaskan Beaufort Sea.

## 6. Conclusions

This study provides the first in-depth estimate of SOC content in sediments along the Yukon coast of the Canadian Beaufort Sea, specifically accounting for the volumes taken up by ground ice in those calculations. SOC was shown to constitute a large proportion of coastal bluffs. It accounted for between 0.5 and 49% by weight of the sediments sampled. This resulted in a mean carbon density of 41 kg C/m<sup>3</sup> in the top 1 m of soil. Mean values were similar among most terrain units (40–53 kg C/m<sup>3</sup>), with the exception of marine deposits (30 kg C/m<sup>3</sup>) having significantly lower values. Across all sites, the top 1 m of soil held 43.8% of total SOC in the soil column, although values ranged more than tenfold across sites due in large part to the large range in bluff heights. In coastal flux studies, the entire soil column must therefore be considered, since failing to do so can result in underestimating carbon transfer by more than half. Terrain units with the lowest overall values of SOC were high bluffs with a high mineral content, while those with the highest SOC values were low bluffs with a thick organic cover. Wedge ice and massive ground ice constituted a significant portion of coastal sediments, with wedge ice accounting for up to 53% of the volume in some cases in the upper, carbon-rich soil layers. The variation of ground ice with depth was less important in low bluffs. If ground ice is not taken into consideration, flux measurements can be overestimated by 19% for SOC and 16% for sediment. The annual flux of organic carbon from coastal erosion along the 282 km of the Yukon Coastal Plain was 0.036 Tg. Extrapolating these results to the area east of the Mackenzie Delta would result in a total coastal flux of organic carbon from the Canadian Beaufort Sea coast of 0.18 Tg/yr. This is almost 3 times more than the values used to date in organic carbon budget calculations (Macdonald et al., 1998; Rachold et al., 2004). The sediment flux for the Yukon section of the Beaufort Sea coast was 1.832 Tg/yr, which is 19% higher than previous estimates due to differences in the length of shoreline considered and probable differences in cliff height estimates. First estimations indicate that up to 12.7% of the organic carbon contributed to the nearshore by coastal erosion is sequestered in the shelf sediments. The rest is either metabolized in the nearshore or exported off the shelf by waves or ice action.

## References

- AMAP (2017). *Snow, water, ice and permafrost in the Arctic (SWIPA) 2017*. Oslo, Norway: Arctic monitoring and assessment programme (AMAP).
- Are, F. E. (1988). Thermal abrasion of sea coasts. *Polar Geography and Geology*, 12(1), 1–157. <https://doi.org/10.1080/10889378809377343>
- Atkinson, D. (2005). Observed storminess patterns and trends in the circum-Arctic coastal regime. *Geo-Marine Letters*, 25(2-3), 98–109. <https://doi.org/10.1007/s00367-004-0191-0>
- Belicka, L. L., & Harvey, H. R. (2009). The sequestration of terrestrial organic carbon in Arctic Ocean sediments: A comparison of methods and implications for regional carbon budgets. *Geochimica et Cosmochimica Acta*, 73(20), 6231–6248. <https://doi.org/10.1016/j.gca.2009.07.020>
- Belicka, L. L., MacDonald, R. W., & Harvey, H. R. (2002). Sources and transport of organic carbon to shelf, slope, and basin surface sediments of the Arctic Ocean. *Deep-Sea Research*, 49(8), 1463–1483. [https://doi.org/10.1016/S0967-0637\(02\)00031-6](https://doi.org/10.1016/S0967-0637(02)00031-6)
- Belicka, L. L., MacDonald, R. W., & Harvey, H. R. (2009). Trace element and molecular markers of organic carbon dynamics along a shelf–basin continuum in sediments of the western Arctic Ocean. *Marine Chemistry*, 115(1-2), 72–85. <https://doi.org/10.1016/j.marchem.2009.06.007>
- Bockheim, J. G., Everett, L. R., Hinkel, K. M., Nelson, F. E., & Brown, J. (1999). Soil organic carbon storage and distribution in Arctic tundra, Barrow, Alaska. *Soil Science Society of America Journal*, 63(4), 934–940. <https://doi.org/10.2136/sssaj1999.634934x>
- Bockheim, J. G., & Hinkel, K. M. (2007). The importance of “deep” organic carbon in permafrost-affected soils of Arctic Alaska. *Soil Science Society of America Journal*, 71(6), 1889–1892. <https://doi.org/10.2136/sssaj2007.0070N>
- Bockheim, J. G., Hinkel, K. M., Eisner, W. R., & Dai, X. Y. (2004). Carbon pools and accumulation rates in an age-series of soils in drained thaw-lake basins, Arctic Alaska. *Soil Science Society of America Journal*, 68(2), 697–704. <https://doi.org/10.2136/sssaj2004.6970>
- Bockheim, J. G., Hinkel, K. M., & Nelson, F. E. (2003). Predicting carbon storage in tundra soils of Arctic Alaska. *Soil Science Society of America Journal*, 67, 648–650. <https://doi.org/10.2136/sssaj2003.9480>
- Bockheim, J. G., & Tarnocai, C. (1998). Recognition of cryoturbation for classifying permafrost-affected soils. *Geoderma*, 81(3-4), 281–293. [https://doi.org/10.1016/S0016-7061\(97\)00115-8](https://doi.org/10.1016/S0016-7061(97)00115-8)
- Bockheim, J. G., Walker, D. A., & Everett, L. R. (1998). Soil carbon distribution in nonacidic and acidic tundra of Arctic Alaska. In R. Lal, J. M. Kimble, R. F. Follett, & B. A. Stewart (Eds.), *Soil Processes and the Carbon Cycle* (pp. 143–155). Boca Raton, FL: CRC Press.
- Bouchard, M. (1974). Surficial geology of Herschel Island, Yukon Territory (MSc. thesis). Montreal, QC: University of Montreal.
- Brown, J., Jorgenson, M. T., Smith, O. P., & Lee, W. (2003). Long-term rates of coastal erosion and carbon input, Elson lagoon, Barrow, Alaska. *Proceedings 8th International Conference on Permafrost* (pp. 101–106). Zurich: University of Zurich.

### Acknowledgments

Financial support was provided to N. Couture by the Fonds québécois de la recherche sur la nature et les technologies (FQRNT), the ArcticNet Network of Centres of Excellence of Canada, the Eben Hobson Fellowship in Arctic Studies. A. M. Irrgang was funded by a grant from the German Federal Environmental Foundation. W. Pollard received support from the Natural Science and Engineering Research Council of Canada. H. Lantuit was funded through the Helmholtz Young Investigators Group “COPER” (grant VH-NG-801). M. Fritz was supported by the Daimler and Benz Foundation (grant 32-02/15). We are grateful to T. Jorgenson and another anonymous reviewer for their helpful comments and suggestions. We wish to express our thanks to the Yukon Territorial Government and the Yukon Parks (Herschel Island Qiqiktaruk Territorial Park). Fieldwork would not have been possible without support from the Polar Continental Shelf Project, the Aurora Research Institute (ARI, Inuvik), and the Northern Scientific Training Program. T. Haltigin, G. De Pascale, G. Manson, H. Meyer, and L. Schirmer assisted in the field. Analytical support from Ute Kuschel at the Alfred Wegener Institute Helmholtz Centre for Polar and Marine Research, Potsdam, is gratefully acknowledged. The georeferenced images used for analysis of the Herschel Island terrain units were provided by J. Ramage. Additional supporting data can be found in the PANGAEA depository at <https://doi.pangaea.de/PANGAEA.884689/PANGAEA.884689> (Couture et al., 2018). This is contribution number 20170202 of Natural Resources Canada.

- Burn, C. R. (1997). Cryostratigraphy, paleogeography, and climate change during the early Holocene warm interval, western Arctic coast, Canada. *Canadian Journal of Earth Sciences*, 34(7), 912–925. <https://doi.org/10.1139/e17-076>
- Burn, C. R., & Zhang, Y. (2009). Permafrost and climate change at Herschel Island (Qikiqtaruaq), Yukon Territory, Canada. *Journal of Geophysical Research*, 114, F02001. <https://doi.org/10.1029/2008JF001087>
- Couture, N. J. (2010). Fluxes of organic carbon from eroding permafrost coasts, Canadian Beaufort Sea (PhD thesis). Retrieved from eScholarship\_McGill (000026878). Montreal, QC: McGill University.
- Couture, N. J., Irrgang, A., Pollard, W., Lantuit, H., & Fritz, M. (2018). Soil organic carbon (SOC) and sediment contents and fluxes for terrain units along the Yukon Coastal Plain, Canada, including corrections for volumetric ground ice contents. <https://doi.pangaea.de/10.1594/PANGAEA.884689>
- Couture, N. J., & Pollard, W. H. (2015). Ground ice determinations along the Yukon coast using a morphological model. In *Proceedings 68th Canadian Geotechnical Conference and 7th Canadian Permafrost Conference* (paper 453, 6 pp.). Richmond, BC: Canadian Geotechnical Society.
- Couture, N. J., & Pollard, W. H. (2017). A model for quantifying ground ice volume, Yukon coast, western Arctic Canada. *Permafrost and Periglacial Processes*, 28(3), 534–542. <https://doi.org/10.1002/ppp.1952>
- Dallimore, S. R., Wolfe, S. A., & Solomon, S. M. (1996). Influence of ground ice and permafrost on coastal evolution, Richards Island, Beaufort Sea coast, N.W.T. *Canadian Journal of Earth Sciences*, 33(5), 664–675. <https://doi.org/10.1139/e96-050>
- de Haas, H., van Weering, T. C. E., & de Stigter, H. (2002). Organic carbon in shelf seas: Sinks or sources, processes and products. *Continental Shelf Research*, 22(5), 691–717. [https://doi.org/10.1016/S0278-4343\(01\)00093-0](https://doi.org/10.1016/S0278-4343(01)00093-0)
- Digital Globe (2014). GeoEye-1 data sheet. Retrieved from [https://dg-cms-uploads-production.s3.amazonaws.com/uploads/document/file/97/DG\\_GeoEye1.pdf](https://dg-cms-uploads-production.s3.amazonaws.com/uploads/document/file/97/DG_GeoEye1.pdf)
- Digital Globe (2016). WorldView-2 data sheet. Retrieved from <https://dg-cms-uploads-production.s3.amazonaws.com/uploads/document/file/98/WorldView2-DS-WV2-rev2.pdf>
- Dittmar, T., & Kattner, G. (2003). The biogeochemistry of the river and shelf ecosystem of the Arctic Ocean: A review. *Marine Chemistry*, 83(3–4), 103–120. [https://doi.org/10.1016/S0304-4203\(03\)00105-1](https://doi.org/10.1016/S0304-4203(03)00105-1)
- Dou, F., Yu, X., Ping, C.-L., Michaelson, G., Guo, L., & Jorgenson, T. (2010). Spatial variations of tundra soil organica carbon along the coastline of northern Alaska. *Geoderma*, 154(3–4), 328–335. <https://doi.org/10.1016/j.geoderma.2009.10.020>
- Dunton, K. H., Weingartner, T., & Carmack, E. C. (2006). The nearshore western Beaufort Sea ecosystem: Circulation and importance of terrestrial carbon in arctic coastal food webs. *Progress in Oceanography*, 71(2–4), 362–378. <https://doi.org/10.1016/j.pocean.2006.09.011>
- Environment Canada (2016). Canadian climate normals. Retrieved from [http://climate.weather.gc.ca/climate\\_normals/](http://climate.weather.gc.ca/climate_normals/)
- Forbes, D. L. (1997). Coastal erosion and nearshore profile variability in the southern Beaufort Sea, Ivvavik National Park, Yukon Territory. *Geological Survey of Canada Open File* (No. 3531). Ottawa, ON: Geological Survey of Canada. doi:<https://doi.org/10.4095/209275>
- Fritz, M., Vonk, J. E., & Lantuit, H. (2017). Collapsing Arctic coastlines. *Nature Climate Change*, 7(1), 6–7. <https://doi.org/10.1038/nclimate3188>
- Fritz, M., Wetterich, S., Schirmeister, L., Meyer, H., Lantuit, H., Preusser, F., & Pollard, W. H. (2012). Eastern Beringia and beyond: late Wisconsinan and Holocene landscape dynamics along the Yukon Coastal Plain, Canada. *Palaeogeography, Palaeoclimatology, Palaeoecology*, 319–320, 28–45. <https://doi.org/10.1016/j.palaeo.2011.12.015>
- Galley, R. J., Babb, D., Ogi, M., Else, B. G. T., Geilfus, N.-X., Crabeck, O., et al. (2016). Replacement of multiyear sea ice and changes in the open water season duration in the Beaufort Sea Since 2004. *Journal of Geophysical Research: Oceans*, 121, 1806–1823. <https://doi.org/10.1002/2015JC011583>
- Gibbs, A. E., & Richmond, B. M. (2015). *National assessment of shoreline change—Historical shoreline change along the North Coast of Alaska, U.S.-Canadian Border to Icy Cape*. U.S. Geological Survey Open File (2015–1048, 96 pp.). Reston, VA: US Geological Survey. <https://doi.org/10.3133/ofr20151048>
- Goñi, M. A., Yunker, M. B., Marcdonald, R. W., & Eglinton, T. I. (2000). Distribution and sources of organic biomarkers in arctic sediments FROM the Mackenzie River and Beaufort shelf. *Marine Chemistry*, 71(1–2), 23–51. [https://doi.org/10.1016/S0304-4203\(00\)00037-2](https://doi.org/10.1016/S0304-4203(00)00037-2)
- Günther, F., Overduin, P. P., Yakshina, I. A., Opel, T., Baranskaya, A. V., & Grigoriev, M. N. (2015). Observing Muostakh disappear: Permafrost thaw subsidence and erosion of a ground-ice-rich island in response to arctic summer warming and sea ice reduction. *The Cryosphere*, 9(1), 151–178. <https://doi.org/10.5194/tc-9-151-2015>
- Harper, J. R. (1990). Morphology of the Canadian Beaufort Sea coast. *Marine Geology*, 91(1–2), 75–91. [https://doi.org/10.1016/0025-3227\(90\)90134-6](https://doi.org/10.1016/0025-3227(90)90134-6)
- Harper, J. R., & Penland, P. S. (1982). *Beaufort Sea sediment dynamics, Contract report to Atlantic Geoscience Centre*. Ottawa, ON: Geological Survey of Canada.
- Harper, J. R., Reimer, P. D., & Collins, A. D. (1985). Canadian Beaufort Sea physical shore zone analysis. *Geological Survey of Canada Open File* (No. 168). Ottawa, ON: Geological Survey of Canada. <https://doi.org/10.4095/130252>
- Harry, D. G., French, H. M., & Pollard, W. H. (1988). Massive ground ice and ice-cored terrain Near Sabine point, Yukon Coastal Plain. *Canadian Journal of Earth Sciences*, 25(11), 1846–1856. <https://doi.org/10.1139/e88-174>
- Hedges, J. I., Keil, R. J., & Benner, R. (1997). What happens to terrestrial organic matter in the ocean? *Organic Geochemistry*, 27(5–6), 195–212. [https://doi.org/10.1016/S0146-6380\(97\)00066-1](https://doi.org/10.1016/S0146-6380(97)00066-1)
- Héquette, A., Ruz, M.-H., & Hill, P. R. (1995). The effects of the Holocene sea-level rise on the evolution of the southeastern coast of the Canadian Beaufort Sea. *Journal of Coastal Research*, 11(2), 494–507.
- Hill, P. R., Blasco, S. M., Harper, J. R., & Fissel, D. B. (1991). Sedimentation on the Canadian Beaufort shelf. *Continental Shelf Research*, 11(8–10), 821–842. [https://doi.org/10.1016/0278-4343\(91\)90081-G](https://doi.org/10.1016/0278-4343(91)90081-G)
- Hilton, R. G., Galy, V., Gaillardet, J., Dellinger, M., Bryant, C., O'Regan, M., et al. (2015). Erosion of organic carbon in the Arctic as a geological carbon dioxide sink. *Nature*, 524(7563), 84–87. <https://doi.org/10.1038/nature14653>
- Hoque, M. A., & Pollard, W. H. (2009). Arctic coastal retreat through block failure. *Canadian Geotechnical Journal*, 46(10), 1103–1115. <https://doi.org/10.1139/T09-058>
- Hoque, M. A., & Pollard, W. H. (2015). Stability of permafrost dominated coastal cliffs in the Arctic. *Polar Science*, 10(1), 79–88. <https://doi.org/10.1016/j.polar.2015.10.004>
- Houghton, R. A. (2007). Balancing the global carbon budget. *Annual Review of Earth and Planetary Sciences*, 35(1), 313–347. <https://doi.org/10.1146/annurev.earth.35.031306.140057>
- Hudak, D. R., & Young, J. M. C. (2002). Storm climatology of the southern Beaufort Sea. *Atmosphere-Ocean*, 40(2), 145–158. <https://doi.org/10.3137/ao.400205>
- Hugelius, G., Strauss, J., Zubrzycki, S., Harden, J. W., Schuur, E. A. G., Ping, C. L., et al. (2014). Estimated stocks of circumpolar permafrost carbon with quantified uncertainty ranges and identified data gaps. *Biogeosciences*, 11(23), 6573–6593. <https://doi.org/10.5194/bg-11-6573-2014>

- Irrgang, A. M., Lantuit, H., Manson, G. K., Günther, F., Grosse, G., Overduin, P. P. (2017). *Quantification of shoreline movements along the Yukon Territory mainland coast between 1951 and 2011*. <https://doi.org/10.1594/PANGAEA.874343>
- Jones, B. M., Arp, C. D., Jorgenson, M. T., Hinkel, K. M., Schmutz, J. A., & Flint, P. L. (2009). Increase in the rate and uniformity of coastline erosion in Arctic Alaska. *Geophysical Research Letters*, *36*, L03503. <https://doi.org/10.1029/2008GL036205>
- Jorgenson, M. T., & Brown, J. (2005). Classification of the Alaskan Beaufort Sea coast and estimation of carbon and sediment inputs from coastal erosion. *Geo-Marine Letters*, *25*(2-3), 69–80. <https://doi.org/10.1007/s00367-004-0188-8>
- Jorgenson, M. T., Macander, M., Jorgenson, J. C., Ping, C.-L., & Harden, J. (2003). Ground ice and carbon characteristics of eroding coastal permafrost at Beaufort Lagoon, northern Alaska. *Proceedings 8th International Conference on Permafrost* (pp. 495-500). Zurich: University of Zurich.
- Kanevskiy, M., Shur, Y., Jorgenson, M. T., Ping, C.-L., Michaelson, G. J., Fortier, D., et al. (2013). Ground ice in the upper permafrost of the Beaufort Sea coast of Alaska. *Cold Regions Science and Technology*, *85*, 56–70. <https://doi.org/10.1016/j.coldregions.2012.08.002>
- Kohnert, K., Serafimovich, A., Hartmann, J., & Sachs, T. (Eds.) (2014). Airborne measurements of methane fluxes in Alaskan and Canadian tundra with the research aircraft Polar 5. *Reports on Polar and Marine Research* (No. 673). Bremerhaven: Alfred Wegener Institute. Hdl:10013/epic.43357.d001
- Kokelj, S. V., Smith, C. A. S., & Burn, C. R. (2002). Physical and chemical characteristics of the active layer and permafrost, Herschel Island, western Arctic coast, Canada. *Permafrost and Periglacial Processes*, *13*(2), 171–185. <https://doi.org/10.1002/ppp.417>
- Koven, C. D., Ringeval, B., Friedlingstein, P., Ciais, P., Cadule, P., Khvorostyanov, D., et al. (2011). Permafrost carbon-climate feedbacks accelerate global warming. *Proceedings of the National Academy of Sciences*, *108*, 14,769–14,774. <https://doi.org/10.1073/pnas.1103910108>
- Lantuit, H., Overduin, P., Couture, N., Wetterich, S., Aré, F., Atkinson, D., et al. (2012). The Arctic coastal dynamics database: A new classification scheme and statistics on Arctic permafrost coastlines. *Estuaries and Coasts*, *35*(2), 383–400. <https://doi.org/10.1007/s12237-010-9362-6>
- Lantuit, H., & Pollard, W. (2005). Temporal stereophotogrammetric analysis of retrogressive thaw slumps on Herschel Island, Yukon Territory. *Natural Hazards and Earth System Sciences*, *5*(3), 413–423. <https://doi.org/10.5194/nhess-5-413-2005>
- Lantuit, H., & Pollard, W. H. (2008). Fifty years of coastal erosion and retrogressive thaw slump activity on Herschel Island, southern Beaufort Sea, Yukon Territory, Canada. *Geomorphology*, *95*(1-2), 84–102. <https://doi.org/10.1016/j.geomorph.2006.07.040>
- Lantuit, H., Rachold, V., Pollard, W. H., Steenhuisen, F., Ødegård, R., & Hubberten, H.-W. (2009). Towards a calculation of organic carbon release from erosion of Arctic coasts using non-fractal coastline datasets. *Marine Geology*, *257*(1-4), 1–10. <https://doi.org/10.1016/j.margeo.2008.10.004>
- Lawrence, M., Pelletier, B. R., & Lacho, G. (1984). Sediment sampling of beaches along the Mackenzie Delta and Tuktoyaktuk Peninsula, Beaufort Sea. In *Geological Survey of Canada Paper* (No. 84-L a, pp. 633–640). Ottawa, ON: Geological Survey of Canada.
- Macdonald, R. W., Naidu, A. S., Yunker, M. B., & Gobeil, C. (2004). The Beaufort Sea: Distribution, sources, fluxes and burial of organic carbon. In R. Stein, & R. W. Macdonald (Eds.), *The Organic Carbon Cycle in the Arctic Ocean* (pp. 177–193). Berlin: Springer.
- Macdonald, R. W., Solomon, S. M., Cranston, R. E., Welch, H. E., Yunker, M. B., & Gobeil, C. (1998). A sediment and organic carbon budget for the Canadian Beaufort shelf. *Marine Geology*, *144*(4), 255–273. [https://doi.org/10.1016/S0025-3227\(97\)00106-0](https://doi.org/10.1016/S0025-3227(97)00106-0)
- Manson, G. K., & Solomon, S. M. (2007). Past and future forcing of Beaufort Sea coastal change. *Atmosphere-Ocean*, *45*(2), 107–122. <https://doi.org/10.3137/ao.450204>
- Markus, T., Stroeve, J. C., & Miller, J. (2009). Recent changes in Arctic sea ice melt onset, freeze up, and melt season length. *Journal of Geophysical Research*, *114*, C12024. <https://doi.org/10.1029/2009JC005436>
- McDonald, B. C., & Lewis, C. P. (1973). Geomorphologic and sedimentologic processes of rivers and coasts, Yukon Coastal Plain. *Environmental-Social Committee, Northern Pipelines Report* (No. 73-39). Ottawa, ON: Geological Survey of Canada.
- McGuire, A. D., Anderson, L. G., Christensen, T. R., Dallimore, S., Guo, L., Hayes, D. J., et al. (2009). Sensitivity of the carbon cycle in the Arctic to climate change. *Ecological Monographs*, *79*(4), 523–555. <https://doi.org/10.1890/08-2025.1>
- Michaelson, G. J., Ping, C. L., & Kimble, J. M. (1996). Carbon storage and distribution in tundra soils of Arctic Alaska, U.S.A. *Arctic and Alpine Research*, *28*(4), 414–424. <https://doi.org/10.2307/1551852>
- Naidu, A. S., Cooper, S. W., Finney, B. P., Macdonald, R. W., Alexander, C., & Semiletov, I. P. (2000). Organic carbon isotope ratios ( $\delta^{13}\text{C}$ ) of Amerasian continental shelf sediments. *International Journal of Earth Sciences*, *89*(3), 522–532. <https://doi.org/10.1007/s005310000121>
- O'Brien, M. C., Macdonald, R. W., Melling, H., & Iseki, K. (2006). Particle fluxes and geochemistry on the Canadian Beaufort shelf: Implications for sediment transport and deposition. *Continental Shelf Research*, *26*(1), 41–81. <https://doi.org/10.1016/j.csr.2005.09.007>
- Obu, J., Lantuit, H., Fritz, M., Grosse, G., Günther, F., Sachs, T., & Helm, V. (2016). *LiDAR elevation data of Yukon Coast and Herschel Island in 2012 and 2013*. <https://doi.org/10.1594/PANGAEA.859046>
- Obu, J., Lantuit, H., Fritz, M., Pollard, W. H., Sachs, T., & Günther, F. (2016). Relation between planimetric and volumetric measurements of permafrost coast erosion: A case study from Herschel Island, western Canadian Arctic. *Polar Research*, *35*(1), 30,313. <https://doi.org/10.3402/polar.v35.30313>
- Obu, J., Lantuit, H., Grosse, G., Günther, F., Sachs, T., Helm, V., & Fritz, M. (2017). Coastal erosion and mass wasting along the Canadian Beaufort Sea based on annual airborne LiDAR elevation data. *Geomorphology*. <https://doi.org/10.1016/j.geomorph.2016.02.014>
- Obu, J., Lantuit, H., Myers-Smith, I., Heim, B., Wolter, J., & Fritz, M. (2017). Effect of terrain characteristics on soil organic carbon and total nitrogen stocks in soils of Herschel Island, western Canadian Arctic. *Permafrost and Periglacial Processes*, *28*(1), 92–107. <https://doi.org/10.1002/ppp.1881>
- Overland, J., Francis, J. A., Hall, R., Hanna, E., Kim, S. J., & Vihma, T. (2015). The melting arctic and midlatitude weather patterns: Are they connected? *Journal of Climate*, *28*(20), 7917–7932. <https://doi.org/10.1175/JCLI-D-14-00822.1>
- Ping, C.-L., Michaelson, G. J., Guo, M. T., Jorgenson, M. T., Kanevskiy, M., Shur, Y., et al. (2011). Soil carbon and material fluxes across the eroding Alaska Beaufort Sea coastline. *Journal of Geophysical Research*, *116*, G02004. <https://doi.org/10.1029/2010JG001588>
- Ping, C.-L., Michaelson, G. J., Jorgenson, M. T., Kimble, J. M., Epstein, H., Romanovsky, V. E., & Walker, D. A. (2008). High stocks of soil organic carbon in the North American Arctic region. *Nature Geoscience*, *1*(9), 615–619. <https://doi.org/10.1038/ngeo284>
- Rachold, V., Eicken, H., Gordeev, V. V., Grigoriev, M. N., Hubberten, H.-W., Lisitzin, A. P., et al. (2004). Modern terrigenous organic carbon input to the Arctic Ocean. In R. Stein, & R. W. Macdonald (Eds.), *The Organic Carbon Cycle in the Arctic Ocean* (pp. 33–55). Berlin: Springer. [https://doi.org/10.1007/978-3-642-18912-8\\_2](https://doi.org/10.1007/978-3-642-18912-8_2)
- Rachold, V., Grigoriev, M. N., Are, F. E., Solomon, S., Reimnitz, E., Kassens, H., & Antonow, M. (2000). Coastal erosion vs. riverine sediment discharge in Arctic shelf seas. *International Journal of Earth Sciences*, *89*(3), 450–460. <https://doi.org/10.1007/s005310000113>
- Rachold, V., Lantuit, H., Couture, N., & Pollard, W. H. (Eds.) (2005). Arctic coastal dynamics: Report of the 5th international workshop. *Berichte zur Polar- und Meeresforschung*, *506*, 1–143.

- Radosavljevic, B., Lantuit, H., Pollard, W., Overduin, P., Couture, N., Sachs, T., et al. (2016). Erosion and flooding—Threats to coastal infrastructure in the Arctic: A case study from Herschel Island, Yukon Territory, Canada. *Estuaries and Coasts*, 39(4), 900–915. <https://doi.org/10.1007/s12237-015-0046-0>
- Ramage, J. L., Irrgang, A. M., Herzsich, U., Morgenstern, A., Couture, N., & Lantuit, H. (2017). Terrain controls on the occurrence of coastal retrogressive thaw slumps along the Yukon coast, Canada. *Journal of Geophysical Research: Earth Surface*, 122, 1619–1634. <https://doi.org/10.1002/2017JF004231>
- Rampton, V. N. (1982). Quaternary geology of the Yukon Coastal Plain. *Geological Survey of Canada Bulletin* (No. 317). Ottawa, ON: Geological Survey of Canada. <https://doi.org/10.4095/111347>
- Reimnitz, E., Graves, S. M., & Barnes, P. W. (1988). *Map showing Beaufort Sea coastal erosion, sediment flux, shoreline evolution, and the erosional shelf profile* (Map I-1182-G, Scale 1:82,000, 22 pp.). Menlo Park, CA: US Geological Survey.
- Schuur, E. A. G., Bockheim, J., Canadell, J. G., Euskirchen, E., Field, C. B., Goryachkin, S. V., et al. (2008). Vulnerability of permafrost carbon to climate change: Implications for the global carbon cycle. *BioScience*, 58, 701–714. <https://doi.org/10.1641/B580807>
- Schuur, E. A. G., McGuire, A. D., Schadel, C., Grosse, G., Harden, J. W., Hayes, D. J., et al. (2015). Climate change and the permafrost carbon feedback. *Nature*, 520, 171–179. <https://doi.org/10.1038/nature14338>
- Serreze, M. C., & Barry, R. G. (2011). Processes and impacts of Arctic amplification: A research synthesis. *Global and Planetary Change*, 77(1–2), 85–96. <https://doi.org/10.1016/j.gloplacha.2011.03.004>
- Smith, C. A. S., Kennedy, C. E., Hargrave, A. E., & McKenna, K. M. (1989). Soil and vegetation of Herschel Island, Yukon Territory. *Yukon Soil Survey Report* (No. 1). Ottawa, ON: Land Resource Research Centre, Agriculture Canada.
- Stein, R., & Macdonald, R. W. (Eds.) (2004). *The organic carbon cycle in the Arctic Ocean*. Berlin: Springer.
- Strauss, J., Schirrmester, L., Grosse, G., Wetterich, S., Ulrich, M., Herzsich, U., & Hubberten, H.-W. (2013). The deep permafrost carbon pool of the Yedoma region in Siberia and Alaska. *Geophysical Research Letters*, 40, GL058088. <https://doi.org/10.1002/2013GL058088>
- Streletskaia, I. D., Vasiliev, A. A., & Vanstein, B. G. (2009). Erosion of sediment and organic carbon from the Kara Sea coast. *Arctic, Antarctic, and Alpine Research*, 41, 79–87. [https://doi.org/10.1657/1938-4246\(08-017\)](https://doi.org/10.1657/1938-4246(08-017))
- Stroeve, J. C., Markus, T., Boisvert, L., Miller, J., & Barrett, A. (2014). Changes in Arctic melt season and implications for sea ice loss. *Geophysical Research Letters*, 41, 1216–1225. <https://doi.org/10.1002/2013GL058951>
- Tarnocai, C. (1998). The amount of organic carbon in various soil orders and ecological provinces in Canada. In R. Lal, J. M. Kimble, R. F. Follett, & B. A. Stewart (Eds.), *Soil processes and the carbon cycle* (pp. 81–92). Boca Raton, FL: CRC Press.
- Tarnocai, C., Canadell, J. G., Schuur, E. A. G., Kuhry, P., Mazhitova, G., & Zimov, S. (2009). Soil organic carbon pools in the northern circumpolar permafrost region. *Global Biogeochemical Cycles*, 23, GB2023. <https://doi.org/10.1029/2008GB003327>
- Tarnocai, C., Kimble, J., & Broll, G. (2003). Determining carbon stocks in cryosols using the northern and mid latitudes soil database. *Proceedings 8th International Conference on Permafrost* (pp. 1129–1134). Zurich: University of Zurich.
- Tarnocai, C., & Lacelle, B. (1996). *The soil organic carbon digital database of Canada*. Ottawa, ON: Research Branch, Agriculture Canada.
- Tarnocai, C., Ping, C.-L., & Kimble, J. (2007). Carbon cycles in the permafrost region of North America. In A. W. King, L. Dilling, G. P. Zimmerman, D. M. Fairman, R. A. Houghton, G. Marland, et al. (Eds.), *The first state of the carbon cycle report (SOCCR): The North American carbon budget and implications for the global carbon cycle* (pp. 127–138). Asheville, NC: National Oceanic and Atmospheric Administration, National Climatic Data Center.
- Thompson, F. (1994). An interpretive manual for reports on granular deposits in the Inuvialuit settlement region: Part of the Inuvialuit final agreement implementation program, task 7 - sand and gravel. In *Part of the Inuvialuit final agreement implementation program task 7—Sand and gravel*, (70 pp.). Ottawa, ON: Indian and Northern Affairs Canada.
- Timmermans, M.-L., & Proshutinsky, A. (2016). (The Arctic) sea surface temperature. In J. Blunden & D. S. Rndt (Eds.), *State of the climate in 2015. Bulletin of the American Meteorological Society*, 97(8), S137–S138.
- Ulrich, M., Grosse, G., Strauss, J., & Schirrmester, L. (2014). Quantifying wedge-ice volumes in yedoma and thermokarst basin deposits. *Permafrost and Periglacial Processes*, 25, 151–161. <https://doi.org/10.1002/ppp.1810>
- Vetrov, A. A., & Romankevich, E. A. (Eds.) (2004). *Carbon cycle in the Russian Arctic seas*. Berlin: Springer.
- Vonk, J. E., Sanchez-Garcia, L., van Dongen, B. E., Alling, V., Kosmach, D., Charkin, A., et al. (2012). Activation of old carbon by erosion of coastal and subsea permafrost in Arctic Siberia. *Nature*, 489, 137–140. <https://doi.org/10.1038/nature1139>
- Wegner, C., Bennett, K. E., de Vernal, A., Forwick, M., Fritz, M., Heikkilä, M., et al. (2015). Variability in transport of terrigenous material on the shelves and the deep Arctic Ocean during the Holocene. *Polar Research*, 34, 24964. <https://doi.org/10.3402/polar.v34.24964>
- Wobus, C., Anderson, R., Overeem, I., Matell, N., Clow, G., & Urban, F. (2011). Thermal erosion of a permafrost coastline: Improving process-based models using time-lapse photography. *Arctic, Antarctic, and Alpine Research*, 43(3), 474–484. <https://doi.org/10.1657/1938-4246-43.3.474>
- Wolfe, S. A., Kotler, E., & Dallimore, S. R. (2001). Surficial characteristics and the distribution of thaw landforms (1970–1999), Shingle Point to Kay Point, Yukon Territory. *Geological Survey of Canada Open File* (No. 4115). Ottawa, ON: Geological Survey of Canada. <https://doi.org/10.4095/212842>
- Yukon Department of Environment (2016). 30 meter Yukon digital elevation model. Retrieved from [http://www.env.gov.yk.ca/publications-maps/geomatics/data/30m\\_dem.php](http://www.env.gov.yk.ca/publications-maps/geomatics/data/30m_dem.php)
- Yunker, M. B., Macdonald, R. W., Cretney, W. J., Fowler, B. R., & McLaughlin, F. A. (1993). Alkane, terpene, and polycyclic aromatic hydrocarbon geochemistry of the Mackenzie River and Mackenzie shelf: Riverine contributions to Beaufort Sea coastal sediment. *Geochimica et Cosmochimica Acta*, 57, 3041–3061. [https://doi.org/10.1016/0016-7037\(93\)90292-5](https://doi.org/10.1016/0016-7037(93)90292-5)
- Yunker, M. B., Macdonald, R. W., Fowler, B. R., Cretney, W. J., Dallimore, S. R., & McLaughlin, F. A. (1991). Geochemistry and fluxes of hydrocarbons to the Beaufort Sea shelf: A multivariate comparison of fluvial inputs and coastal erosion of peat using principal components analysis. *Geochimica et Cosmochimica Acta*, 55, 255–213. [https://doi.org/10.1016/0016-7037\(91\)90416-3](https://doi.org/10.1016/0016-7037(91)90416-3)
- Yunker, M. B., McLaughlin, F. A., Fowler, B. R., Smyth, T. A., Cretney, W. J., Macdonald, R. W., & McCullough, D. (1990). Hydrocarbon determinations; Mackenzie River and Beaufort Sea shoreline peat samples. *Canadian Data Report of Hydrography and Ocean Sciences* (NOGAP B6; Volume 7: 60). Ottawa, ON: Department of Fisheries and Oceans.
- Zhang, K., Douglas, B. C., & Leatherman, S. P. (2004). Global warming and coastal erosion. *Climatic Change*, 64, 41–58. <https://doi.org/10.1023/b:clim.0000024690.32682.48>
- Zimov, S. A., Schuur, E. A. G., & Chapin, F. S. III (2006). Permafrost and the global carbon budget. *Science*, 312, 1612–1613. <https://doi.org/10.1126/science.1128908>